

1 Aerosol and Precipitation Chemistry in the Southwestern United States: Spatiotemporal Trends  
2 and Interrelationships

3  
4 A. Sorooshian<sup>1,2</sup>, T. Shingler<sup>1</sup>, A. Harpold<sup>3,4</sup>, C. W. Feagles<sup>1</sup>, T. Meixner<sup>3</sup>, P. D. Brooks<sup>3</sup>

5  
6 [1] {Department of Chemical and Environmental Engineering, University of Arizona, Tucson,  
7 Arizona, USA }

8 [2] {Department of Atmospheric Sciences, University of Arizona, Tucson, Arizona, USA }

9 [3] {Department of Hydrology and Water Resources, University of Arizona, Tucson, Arizona,  
10 USA }

11 [4] {Institute of Arctic and Alpine Research, University of Colorado Boulder, Boulder,  
12 Colorado, USA }

13  
14 Correspondence to: A. Sorooshian (armin@email.arizona.edu)

15  
16 **Abstract**

17  
18 This study characterizes the spatial and temporal patterns of aerosol and precipitation  
19 composition at six sites across the United States Southwest between 1995 and 2010. Precipitation  
20 accumulation occurs mostly during the wintertime (December - February) and during the  
21 monsoon season (July - September). Rain and snow pH levels are usually between 5 – 6, with  
22 crustal-derived species playing a major role in acid neutralization. These species ( $\text{Ca}^{2+}$ ,  $\text{Mg}^{2+}$ ,  
23  $\text{K}^+$ ,  $\text{Na}^+$ ) exhibit their highest concentrations between March and June in both  $\text{PM}_{2.5}$  and  
24 precipitation due mostly to dust. Crustal-derived species concentrations in precipitation exhibit  
25 positive relationships with  $\text{SO}_4^{2-}$ ,  $\text{NO}_3^-$ , and  $\text{Cl}^-$ , suggesting that acidic gases likely react with and  
26 partition to either crustal particles or hydrometeors enriched with crustal constituents.  
27 Concentrations of particulate  $\text{SO}_4^{2-}$  show a statistically significant correlation with rain  $\text{SO}_4^{2-}$   
28 unlike snow  $\text{SO}_4^{2-}$ , which may be related to some combination of the vertical distribution of  
29  $\text{SO}_4^{2-}$  (and precursors) and the varying degree to which  $\text{SO}_4^{2-}$ -enriched particles act as cloud  
30 condensation nuclei versus ice nuclei in the region. The coarse:fine aerosol mass ratio was  
31 correlated with crustal species concentrations in snow unlike rain, suggestive of a preferential  
32 role of coarse particles (mainly dust) as ice nuclei in the region. Precipitation  $\text{NO}_3^-:\text{SO}_4^{2-}$  ratios  
33 exhibit the following features with potential explanations discussed: (i) they are higher in  
34 precipitation as compared to  $\text{PM}_{2.5}$ ; (ii) they exhibit the opposite annual cycle compared to  
35 particulate  $\text{NO}_3^-:\text{SO}_4^{2-}$  ratios; and (iii) they are higher in snow relative to rain during the  
36 wintertime. Long-term trend analysis for the monsoon season shows that the  $\text{NO}_3^-:\text{SO}_4^{2-}$  ratio in  
37 rain increased at the majority of sites due mostly to air pollution regulations of  $\text{SO}_4^{2-}$  precursors.

47 **1 Introduction**

48

49 The southwestern United States is experiencing rapid population growth, land-use change,  
50 drought, and variability in precipitation and water availability (Woodhouse et al., 2010; Cayan et  
51 al., 2010; Seager and Vecchi, 2010; Harpold et al., 2012), which both affect and are affected by  
52 the region's aerosol particles and precipitation. Ongoing changes in the Southwest's climate are  
53 reducing the relative contributions of winter snow versus summer rain to the annual water  
54 balance (Cayan et al., 2010) and shortening the duration of snow cover and melt (Harpold et al.,  
55 2012). Although chemical relationships between particulate matter and precipitation have been  
56 studied in a wide range of environments, few locations exhibit as wide a range of sensitivity to  
57 atmospheric chemistry as the Southwest. For example, dust deposition in seasonal snowpacks  
58 increases melt rate during spring in the mountains of Colorado (Painter et al., 2007). The amount  
59 of fine and coarse aerosol particles may also alter the amount and spatial distribution of potential  
60 rain or snow via their role as cloud condensation nuclei (CCN) and ice nuclei (IN), respectively  
61 (e.g Rosenfeld and Givati, 2006). In both desert and montane ecosystems, the deposition of  
62 nitrate and sulfate have been shown to be acidifying agents for aquatic ecosystems resources  
63 (e.g. Fenn et al., 2003), while excess nitrogen in precipitation has altered plant-soil nutrient  
64 relations and induced directional biological shifts in ecosystems (Fenn et al., 1998; Baron et al.,  
65 2000; Wolfe et al., 2003; Neff et al., 2008). Consequently, the composition and acidity of wet  
66 deposition in the Southwest have critical effects on terrestrial and aquatic ecosystems.

67

68 Precipitation chemistry is governed largely by the composition of the seeds of warm cloud  
69 droplets (cloud condensation nuclei, CCN) and snow (ice nuclei, IN), and gases and particles that  
70 deposit to these hydrometeors. There have been limited attempts to examine precipitation  
71 chemistry in relation to air mass source origins and particulate matter composition in the  
72 Southwest. Hutchings et al. (2009) focused on monsoon clouds near Flagstaff, Arizona and  
73 suggested that windblown soils serve as CCN and can be found in cloud water. It is widely  
74 accepted that dust particles act as both CCN (Levin et al., 1996; Rosenfeld et al., 2001; Koehler  
75 et al., 2007) and IN (Isono and Ikebe, 1960; Kumai, 1961; Twohy and Gandrud, 1998;  
76 Heintzenberg et al., 1996; DeMott et al., 2003a/b; Sassen et al., 2003; Cziczo et al., 2004;  
77 Koehler et al., 2007; Prenni et al., 2009; Zimmermann et al., 2008), which is important for the  
78 Southwest as it has the highest dust concentrations in the United States (e.g. Malm et al., 2004).  
79 This is assisted by disrupted soils from agricultural activity, vehicles, construction, grazing, and  
80 mining operations (Schlesinger et al., 1990; Neff et al., 2005; Fernandez et al., 2008; Csavina et  
81 al., 2012). Atmospheric dust not only originates from regional sources in the Southwest and  
82 Mexico, but it can also be transported from distant regions such as Asia, especially in spring  
83 months (VanCuren and Cahill, 2002; Jaffe et al., 2003; Wells et al., 2007; Kavouras et al., 2009).  
84 In addition to dust, the region is impacted by diverse anthropogenic and biogenic sources with  
85 the relative strength of each of these sources being sensitive to meteorological and seasonal  
86 factors.

87

88 The goal of this work is to examine co-located aerosol and wet deposition chemical  
89 measurements at six Southwest sites with an aim to characterize their spatiotemporal trends and  
90 interrelationships. The analysis specifically aims to address the following questions: (i) What is  
91 the annual profile of rain/snow water accumulation, precipitation pH, and composition of  
92 precipitation and aerosol particles?; (ii) What species are best correlated with each other in rain

93 and snow?; (iii) What species are most influential towards rain and snow water pH?; (iv) How  
94 well-correlated are common species measured in aerosol and precipitation samples?; (v) What is  
95 the nature of the nitrate:sulfate ratio in precipitation and aerosol particles? and (vi) How have  
96 aerosol and precipitation species concentrations changed between 1995 and 2010?

## 98 **2 Data**

### 99 **2.1 Aerosol data**

100  
101 Aerosol composition data were obtained from the Interagency Monitoring of Protected Visual  
102 Environments (IMPROVE) network (Malm et al., 1994, 2004;  
103 <http://views.cira.colostate.edu/web/>). IMPROVE aerosol monitoring stations are located  
104 primarily in National Parks and Wilderness Areas and contain samplers that collect ambient  
105 aerosol on filters over a period of 24 h, typically every third day. Prior to 2000, sampling was  
106 conducted twice each week with a 24 h duration per sample. The change in sampling frequency  
107 in 2000 is not expected to bias the results over the monthly and seasonal time scales of interest in  
108 this study. Collected samples are analyzed for ions, metals, and both organic carbon (OC) and  
109 elemental carbon (EC). Ammonium is not routinely measured in the IMPROVE program and  
110 thus its concentrations in precipitation are only discussed. Sampling protocols and additional  
111 details are provided elsewhere  
112 ([http://vista.cira.colostate.edu/improve/Publications/SOPs/UCDavis\\_SOPs/IMPROVE\\_SOPs.ht](http://vista.cira.colostate.edu/improve/Publications/SOPs/UCDavis_SOPs/IMPROVE_SOPs.htm)  
113 [m](http://vista.cira.colostate.edu/improve/Publications/SOPs/UCDavis_SOPs/IMPROVE_SOPs.htm)). Nitrate is vulnerable to measurement artifacts and this issue is minimized via the use of an  
114 annular denuder (to remove nitric acid, HNO<sub>3</sub>) and nylon filters as compared to Teflon to prevent  
115 NO<sub>3</sub><sup>-</sup> loss via recapture of volatilized HNO<sub>3</sub> (Ames and Malm, 2001; Yu et al., 2005). This study  
116 uses data from six sites summarized in Table 1 and Fig. 1 in terms of location, altitude, and range  
117 of dates for which data are examined. Specific species concentrations discussed in this study are  
118 from the “fine” fraction of aerosol, PM<sub>2.5</sub>, while total mass concentrations are also reported for  
119 the “coarse” fraction, defined as PM<sub>10</sub> – PM<sub>2.5</sub>. Among the elemental measurements, x-ray  
120 fluorescence (XRF) is used for iron (Fe) and heavier elements while particle-induced x-ray  
121 emission (PIXE) is used for elements ranging from sodium (Na) to manganese (Mn). Fine soil is  
122 discussed in this work and is calculated from IMPROVE tracer concentrations using the  
123 following equation (Malm et al., 2004):

$$124$$
$$125 \text{ Fine Soil } (\mu\text{g m}^{-3}) = 2.2[\text{Al}] + 2.49[\text{Si}] + 1.63[\text{Ca}] + 2.42[\text{Fe}] + 1.94[\text{Ti}] \quad (1)$$
$$126$$

127 Statistical methods used to analyze IMPROVE and the precipitation data below are briefly  
128 summarized in the Supplementary Material.

### 130 **2.2 Precipitation data**

131  
132 Precipitation chemistry and pH data are reported from six sites (Table 1 and Fig. 1) from the  
133 National Atmospheric Deposition Program (NADP) National Trends Network (NTN)  
134 (<http://nadp.sws.uiuc.edu/data/ntndata.aspx>) that span a gradient of summer rain being dominant  
135 to roughly equal contributions of summer rain and winter snow. These six stations are co-located  
136 with the IMPROVE stations. Each of the sites has a wet deposition collector that is only open  
137 during precipitation events. Weekly samples are obtained in cleaned containers, the contents of  
138 which are sent to the Central Analytical Laboratory (CAL) at the Illinois State Water Survey

139 (ISWS) where the following measurements are conducted: free acidity (i.e. pH), conductance,  
140 and concentrations of ammonium ( $\text{NH}_4^+$ ), calcium ( $\text{Ca}^{2+}$ ), chloride ( $\text{Cl}^-$ ), magnesium ( $\text{Mg}^{2+}$ ),  
141 nitrate ( $\text{NO}_3^-$ ), potassium ( $\text{K}^+$ ), sodium ( $\text{Na}^+$ ), and sulfate ( $\text{SO}_4^{2-}$ ). Data that were obtained from  
142 the NADP data repository have undergone quality control and assurance protocols  
143 (<http://nadp.sws.uiuc.edu/data/ntndata.aspx>). Data have been categorized to separate rain and  
144 snow, with no instances of rain-snow mixtures included in the analysis. Since sample handling  
145 procedures at all NADP/NTN sites changed substantially on 11 January 1994, data are only used  
146 beginning in 1 January 1995 or the first day of January in another year if data collection began in  
147 the middle of a year.

148

### 149 **2.3 Remote sensing data**

150

151 Regional maps of ultraviolet aerosol index (UV AI) were developed using data from the Ozone  
152 Monitoring Instrument (OMI) for the period between 2005 – 2008. Data were obtained at a  
153 resolution  $1^\circ \times 1.25^\circ$  using a minimum threshold value of 0.5 (Hsu et al., 1999). The UV AI  
154 parameter serves as a proxy for absorbing aerosol particles (Torres et al., 1998), which are  
155 predominantly comprised of smoke and dust. UV AI is used here as a proxy for dust owing to its  
156 greater abundance relative to smoke in the region over the time scales examined in this work.

157

### 158 **3 Site descriptions**

159

160 The six sites studied represent areas throughout the southwestern United States influenced by  
161 varying degrees of pollution and meteorological conditions (Fig. 1). Organ Pipe National  
162 Monument is the lowest altitude site ( $\sim 500$  m ASL) and the closest to marine-derived emissions  
163 from the Pacific Ocean. Organ Pipe is approximately 16 km north of the US-Mexico border in  
164 southern Arizona. Anthropogenic pollution sources include the towns of Sonoyta, Mexico  
165 (population  $\sim 15,000$ ,  $\sim 10$  km south; <http://www.inegi.org.mx/default.aspx>) and Ajo, Arizona  
166 (city population  $\sim 3,500$ ,  $\sim 36$  km north; US Census Bureau 2010). Chiricahua National  
167 Monument ( $\sim 1,560$  m ASL) is located in the Chiricahua Mountains in southeastern Arizona,  
168 approximately 18 km west of the Arizona-New Mexico border. Willcox, Arizona (city  
169 population  $\sim 3,800$ ; US Census Bureau 2010) is located 55 km west of Chiricahua and contains  
170 the Willcox Playa and the Apache Power Station, which is a coal-fired power station. Sierra  
171 Vista, Arizona (city population  $\sim 44,000$ ; US Census Bureau 2010) is located 97 km to the  
172 southwest of Chiricahua. The largest source of major urban pollution is Tucson, Arizona (city  
173 population  $\sim 520,000$ ; US Census Bureau 2010), which is 150 km to the west of Chiricahua. This  
174 site can also be influenced by copper smelter emissions from the Mexican towns of Cananea and  
175 Nacozari (140 km and 180 km south of Chiricahua, respectively).

176

177 The Gila stations ( $\sim 1,775$  m ASL) are in southwestern New Mexico. The nearest town is Silver  
178 City, New Mexico (city population  $\sim 10,000$ ; US Census Bureau 2010), which includes a  
179 number of large open-pit copper mining operations. Lordsburg, New Mexico (city population  $\sim$   
180  $2,800$ ; US Census Bureau 2010) is 70 km to the southwest and is home to the Lordsburg  
181 Generating Station, a natural-gas fired power station. A major source of urban pollution is Las  
182 Cruces, New Mexico (city population  $\sim 98,000$ ; US Census Bureau 2010), which is 170 km to  
183 the southeast. The Bandelier National Monument stations ( $\sim 1,990$  m ASL) are located in  
184 northern central New Mexico. Bandelier is situated near the major population centers of Santa

185 Fe, New Mexico (city population ~ 68,000; US Census Bureau 2010) and Albuquerque (city  
186 population ~ 633,000; US Census Bureau 2010). Albuquerque is home to two natural gas-fired  
187 power stations. The Reeves Generating Station is 72 km to the southwest and the Delta-Person  
188 Generating Station is 88 km to the southwest.

189  
190 Mesa Verde National Park (~ 2,165 m ASL) is in southwestern Colorado. It is close to the  
191 Colorado cities of Cortez (city population ~ 8,500; US Census Bureau 2010) and Durango (city  
192 population ~ 17,000; US Census Bureau 2010). Approximately 57 km to the southeast is the city  
193 of Farmington (city population ~ 46,000; US Census Bureau 2010), which contains two large  
194 coal-fired powers stations. The San Juan Generating Station and the Four Corners Power Plant  
195 are 46 km and 53 km south of Mesa Verde, respectively. Bryce Canyon National Park is the  
196 highest altitude site (~ 2,480 m ASL) and is in southern Utah. Cedar City (city population ~  
197 29,000; US Census Bureau 2010) is located 80 km to the west and St. George (city population ~  
198 70,000; US Census Bureau 2010) is located 127 km to the southwest. The Navajo Generating  
199 Station is located 104 km to the southeast in Arizona and is a large coal-fired power station.

200

## 201 **4 Results**

### 202 **4.1 Air mass source regions**

203

204 Figure 2 summarizes the representative air mass source regions for each site as a function of  
205 season using three-day back-trajectory data from the NOAA HYSPLIT Model (Draxler and  
206 Rolph, 2012). Four seasons are defined in this study as follows: December – February (DJF),  
207 March – June (MAMJ), July – September (JAS), October – November (ON). The MAMJ season  
208 is meant to include the months with strongest dust influence, while JAS represents the monsoon  
209 season. Air masses from the Pacific Ocean influence all sites, with the strongest influence on  
210 Organ Pipe due to its proximity to the ocean. The three southernmost sites (Organ Pipe,  
211 Chiricahua, Gila) tend to exhibit similar trajectory frequency patterns relative to the three sites  
212 that are farther north. The former three stations that are closest to the US-Mexico border are most  
213 influenced by crustal emissions from the Sonoran Desert, dry lake beds such as Laguna Salada  
214 (southwest of Yuma, Arizona), the Chihuahuan Desert and a network of playas and alluvial,  
215 lacustrine, and aeolian sediments near the Mimbres Basin by southwestern New Mexico. The  
216 major seasonal difference at the easternmost sites is that the MAMJ trajectories originate farthest  
217 from the west, while JAS tends to coincide with more influence from towards the Gulf of  
218 Mexico. This is consistent with the arrival of monsoon moisture from the Gulf of Mexico during  
219 this time of year (Adams and Comrie, 1997; Higgins et al., 1997). Mesa Verde and Bryce  
220 Canyon exhibit similar trajectory frequency maps and receive more influence from the northwest  
221 direction as compared to the other sites. The DJF and ON seasons are characterized by being  
222 influenced by air with the smallest range of distance away from the study sites owing to  
223 meteorological conditions suppressing transport relative to the other two seasons. The majority  
224 of the back-trajectories include the Phoenix metropolitan area, which have previously been  
225 linked to enhanced levels of anthropogenic species (e.g. sulfate, lead, copper, cadmium) in cloud  
226 water more than 200 km to the north in Flagstaff, Arizona (Hutchings et al., 2009).

227

### 228 **4.2 Aerosol data**

229

230 The majority of the aerosol mass at the study sites resides in the coarse fraction, which is due to  
231 the strong influence of dust (Fig. 3). The two lowest altitude sites (Organ Pipe and Chiricahua)  
232 exhibit the highest coarse aerosol concentrations on an annual basis with their concentration  
233 peaks in July ( $9.55 \pm 7.41 \mu\text{g m}^{-3}$ ) and May ( $8.97 \pm 3.74 \mu\text{g m}^{-3}$ ), respectively. Owing to Organ  
234 Pipe's lower altitude and closer proximity to dust and sea salt sources, it exhibits higher  
235 concentrations year-round with fairly sustained average coarse aerosol concentrations between  
236 April and September ( $8.25 - 9.55 \mu\text{g m}^{-3}$ ). The spatial and temporal patterns in coarse aerosol  
237 concentrations across the Southwest are consistent with seasonal UV AI maps (Fig. 4). The  
238 highest regional values occur during MAMJ, followed by JAS, ON, and then DJF. The sites co-  
239 located with the highest and lowest year-round UV AI levels are Organ Pipe and Bryce Canyon,  
240 respectively. A consistent feature at all sites except Organ Pipe is that the ratio of coarse:fine  
241 aerosol mass is highest during MAMJ (Fig. 5); this ratio can be used as a measure of when  
242 coarse dust aerosol influence is strongest from local sources (Tong et al., 2012). The average  
243 coarse:fine ratio at Organ Pipe is highest in DJF (1.98); the different behavior of this ratio at this  
244 site may be due to its proximity to marine-derived sea salt emissions (Fig. 2).

245  
246  $\text{PM}_{2.5}$  concentrations peak between May and July for the six sites, indicative of sources and  
247 production mechanisms (i.e. gas to particle conversion) that differ from coarse aerosol in the  
248 region. The most abundant contributors to  $\text{PM}_{2.5}$  are fine soil, organic carbon (OC),  $\text{SO}_4^{2-}$ , and  
249  $\text{NO}_3^-$  (Fig. 6). Fine soil levels are highest in the spring months (April - May) owing largely to dry  
250 conditions, high wind speeds, and also the highest frequency of transported Asian dust  
251 (VanCuren and Cahill, 2002; Jaffe et al., 2003; Wells et al., 2007; Kavouras et al., 2009; Tong et  
252 al., 2012). The contributions of Ca, Mg, and Na to  $\text{PM}_{2.5}$  are highest during MAMJ due most  
253 likely to fine soil emissions (Fig. 5). Potassium is associated with crustal matter and biomass  
254 burning emissions, and its highest concentrations and mass fractions occur during MAMJ.  
255 Although no direct measurement of organic carbon (OC) is available in the precipitation datasets,  
256 OC in the  $\text{PM}_{2.5}$  fraction is still examined owing to its significant contribution ranging from 10 -  
257 29% depending on the site and season (Fig. 5); note that the inorganic aerosol constituents  
258 examined account for between 28 - 47% of  $\text{PM}_{2.5}$ . Organic carbon has a variety of sources in the  
259 Southwest where it is produced via both direct emission and secondary production processes  
260 from sources including biomass burning, biological particles, biogenic emissions such as  
261 isoprene, combustion, meat cooking, plant debris, and dust (Bench et al., 2007; Schichtel et al.,  
262 2008; Holden et al., 2011; Sorooshian et al., 2011; Cahill et al., 2013; Youn et al., 2013).  
263 Although the atmospheric mixing height is largest between May - July in the region (Sorooshian  
264 et al., 2011), OC concentrations are the highest at all the sites during this time suggestive of the  
265 influence of biomass burning and secondary OC production. Sulfate production is enhanced  
266 during moist conditions, which occurs during the monsoon months in the Southwest. As a result,  
267 maximum concentrations (Fig. 6) and mass fractions (Fig. 5) for  $\text{SO}_4^{2-}$  are observed during JAS.

268  
269 Nitrate is a marker for anthropogenic emissions as it often increases in concentration with  
270 decreasing mixing height in the winter months and because it is thermodynamically more stable  
271 in colder conditions; however, it is also associated with larger particles in the fine mode owing to  
272 reactions of  $\text{HNO}_3$  (or precursors) with dust and sea salt (Malm et al., 2003; Lee et al., 2004,  
273 2008). As a result,  $\text{NO}_3^-$  exhibits a bimodal concentration profile with a peak in the winter  
274 months and during the spring months when soil dust is most abundant. Nitrate mass fractions are  
275 usually highest in DJF. Chloride exhibits peak concentrations in various months (March, May,

276 June, October – December) depending on the site. Maximum concentrations observed at the  
277 majority of sites between March and June likely originate from a combination of crustal-derived  
278 particles and other sources such as biomass burning (e.g. Wonaschütz et al., 2011). Chloride is  
279 especially enhanced at Organ Pipe due to marine-derived sea salt, which is supported by higher  
280 mass fractions of Cl<sup>-</sup> and Na at this site relative to others (Fig. 5).

281

## 282 **4.3 Precipitation data**

### 283 **4.3.1 Annual rain and snow accumulation profiles**

284

285 Precipitation falls in two major modes (Fig. 7). The first is during DJF mostly as a result of  
286 Pacific Ocean frontal storms. These storms provide snow to high altitude sites and warm rain to  
287 lower altitude sites. The second mode is the summertime monsoon rainfall that typically occurs  
288 between July and October. The lowest altitude site, Organ Pipe, was the only one to have no  
289 snow data recorded. The next lowest altitude site, Chiricahua, has relatively similar amounts of  
290 snow and rain during the DJF period. This site also is characterized by major enhancements in  
291 precipitation during the monsoon season, with the two highest amounts in July and August (71  
292 mm and 90 mm, respectively). The relative amount of snow in DJF relative to rain during JAS  
293 increases as a function of altitude and distance to the north for the other sites: Bryce Canyon >  
294 Mesa Verde > Bandelier > Gila Cliffs. Table S1 (Supplementary Material) reports more specific  
295 statistics for precipitation data for each month and site. July and August are the months with the  
296 most frequent rain days (~ 5 – 12 depending on the site). The month with most frequent snow  
297 days (~ 1 – 7 days, depending on the site) varied between December and February.

298

### 299 **4.3.2 Annual composition and pH profiles**

300

301 Rain pH levels are generally highest during MAMJ (Fig. 8) with annual averages at the sites  
302 ranging between 5 and 6. Cloud water pH levels at a high-altitude site near Flagstaff, Arizona  
303 ranged between 5.12 – 6.66, and were said to be high due to crustal acid-neutralizing  
304 components (Hutchings et al., 2009). Studies in other regions have shown that carbonate bases  
305 associated with dust can neutralize acidic inputs to precipitation and increase pH (Schwikowski  
306 et al., 1995; Loye-Pilot and Morelli, 1988; Williams and Melack, 1991; Rhoades et al., 2010).  
307 Examples of regions with higher pH values (> 6) than those in the Southwest, mostly due to  
308 alkaline species (e.g. ammonium from agriculture and calcium carbonate from soil dust), are  
309 India (Khemani et al., 1987; Kulshrestha et al., 2005; Mouli et al., 2005), Jordan (Al-Khashman,  
310 2009), Niger (Galy-Lacaux et al., 2009), Spain (Avila et al., 1997, 1998), Israel (Herut et al.,  
311 2000), Phnom Penh (Cambodia), Ulaanbaatar (Mongolia) and Jiwozi and Shuzhan in China  
312 (EANET Executive Summary, 2011). Regions with lower rain pH values include the eastern  
313 United States, eastern Mediterranean, Canada, Turkey, Thailand, Singapore, and China (Granat  
314 et al., 1996; Al-Momani et al., 1997; Sirois et al., 2000; Balasubramanian et al., 2001; Qin and  
315 Huang, 2001; Basak and Alagha, 2004; Likens, 2007). It is cautioned that the temporal range of  
316 measurements is varied for these studies, which can affect pH comparisons; for example,  
317 reductions in sulfur dioxide (SO<sub>2</sub>) emissions in the Southwest over the last several years have  
318 resulted in reduced particulate sulfate levels (Matichuk et al., 2006; Sorooshian et al., 2011),  
319 which influences precipitation pH.

320

321 To more closely examine when dust impacts precipitation in the Southwest,  $\text{Ca}^{2+}$  and  $\text{Mg}^{2+}$  are  
322 used as rain tracer species (e.g. Stoorvogel et al., 1997; Reynolds et al., 2001; Rhoades et al.,  
323 2010); other crustal-derived rain constituents such as  $\text{K}^+$  and  $\text{Na}^+/\text{Cl}^-$  are not used as they likely  
324 have contributions from biomass burning and sea salt, respectively. The rain water concentration  
325 sum of  $\text{Ca}^{2+}$  and  $\text{Mg}^{2+}$  is highest at all sites during the months of April – June (Fig. 8), which  
326 coincides with the highest levels of dust according to IMPROVE and satellite data (Fig. 3 - 6).  
327 Organ Pipe and Mesa Verde exhibit the highest levels of fine soil between April - May, which  
328 presumably explains why they also have the highest rain pH in those months. Rain  $\text{Cl}^-$  and  $\text{K}^+$   
329 concentrations are also highest during MAMJ, likely due to crustal emissions (dust and sea salt);  
330  $\text{Cl}^-$  is most abundant at Organ Pipe for nearly the entire year due to sea salt from marine-derived  
331 air masses that impact the site year-round (Fig. 2). Nitrate and  $\text{SO}_4^{2-}$  exhibit different annual  
332 concentration profiles in precipitation as compared to  $\text{PM}_{2.5}$  for reasons that will be discussed  
333 subsequently.

334  
335 Figure S1 (Supplementary Material) shows annual cycles for snow water constituent  
336 concentrations. Annual snow pH values range between 5 and 6 at the various sites, similar to rain  
337 water. Snow pH and the concentration sum of  $\text{Ca}^{2+}$  and  $\text{Mg}^{2+}$  are highest between March and  
338 May for three sites (Gila Wilderness, Chiricahua, Mesa Verde), and between September and  
339 October for Bryce Canyon and Bandelier. The rest of the species exhibit their highest  
340 concentrations in a wide range of months depending on the site.

#### 341 342 **4.3.3 Precipitation species mass fractions**

343  
344 Either  $\text{Cl}^-$ ,  $\text{SO}_4^{2-}$ , or  $\text{NO}_3^-$  is the dominant rain anion on a mass basis depending on the site and  
345 season (Fig. 9). Chloride exhibits the highest anion mass fraction in Organ Pipe rain during DJF  
346 (29%) due largely to sea salt. Nitrate is the dominant anion at Organ Pipe during JAS (44%) and  
347 ON (39%), while all three anions are nearly equivalent contributors during MAMJ (20 – 24%).  
348 Sulfate and  $\text{NO}_3^-$  exhibit the highest anion mass fractions in rain at the other sites with a  
349 consistent trend being that  $\text{NO}_3^-$  accounts for the highest mass fraction in JAS and MAMJ. The  
350 highest cation mass fraction in rain was usually for  $\text{Ca}^{2+}$  (6 – 27%) at all six sites and seasons  
351 with the following exceptions:  $\text{NH}_4^+$  (10 – 13%; Bandelier DJF, Chiricahua DJF/ON, Organ Pipe  
352 JAS);  $\text{Na}^+$  (14 – 18%; Organ Pipe DJF/MAMJ). Snow mass fraction data are only shown for DJF  
353 in Fig. 9 due to insufficient data in other months. The highest snow cation mass fraction in DJF  
354 was always for  $\text{Ca}^{2+}$  (9 – 19%), followed by either  $\text{NH}_4^+$  (5 – 7%),  $\text{K}^+$  (8%), or  $\text{Na}^+$  (9%). The  
355 anion with the highest mass fraction in snow was usually  $\text{NO}_3^-$  (28 – 49%), followed by  $\text{SO}_4^{2-}$   
356 (19 – 29%), and  $\text{Cl}^-$  (4 – 14%).

357  
358 In other regions such as those associated with the Acid Deposition Monitoring Network in East  
359 Asia (EANET; EANET Executive Summary, 2011), the Tibetan Plateau, Canada, Spain, India,  
360 and Israel, the dominant precipitation cation has been reported to be either  $\text{Ca}^{2+}$ ,  $\text{Na}^+$ , or  $\text{NH}_4^+$   
361 (Avila et al., 1998; Herut et al., 2000; Kulshrestha et al., 2005; Zhang et al., 2007 and references  
362 therein; Aherne et al., 2010; Yi et al., 2010; Zhang et al., 2012). Those studies also showed that  
363  $\text{SO}_4^{2-}$  was the dominant anion, which may be due to significant anthropogenic influence in those  
364 studies; the one exception was in western Canada where marine-influenced air promoted  $\text{Cl}^-$  to  
365 be the dominant anion. Calcium and  $\text{Cl}^-$  were shown to be the dominant cation and anion,  
366 respectively, in Jordan rain water (Al-Khashman, 2009). Consistent with our results, Hutchings

367 et al. (2009) showed that  $\text{NO}_3^-$  was frequently more abundant than  $\text{SO}_4^{2-}$  in northern Arizona  
368 monsoon cloud water; however, they also showed that  $\text{NH}_4^+$  was the dominant cation. San  
369 Joaquin Valley and Sacramento fog water in California exhibited high  $\text{NO}_3^-$ :  $\text{SO}_4^{2-}$  concentration  
370 ratios (equivalent/equivalent) of 4.8 and 8.6, respectively, due to the influence of agricultural  
371 emissions (Collett et al., 2002). It is cautioned again that such comparisons are sensitive to the  
372 time span of data examined due to reasons such as varying air quality regulations at different  
373 locations and times. Significant changes in the relative amounts of  $\text{SO}_4^{2-}$  and  $\text{NO}_3^-$  have been  
374 observed in the United States since the 1980s (e.g. Butler and Likens, 1991; Lynch et al., 1995;  
375 Nilles and Conley, 2001; Butler et al., 2001; EPA, 2003).

## 376 **5 Discussion**

### 377 **5.1 Sources of precipitation species**

#### 378 **5.1.1 Interrelationships between precipitation species concentrations**

380  
381 Correlation matrices for rain and snow chemical concentrations are used to provide more support  
382 for common sources of species, using Organ Pipe and Bandelier as representative examples for  
383 rain and snow, respectively (Table 2). Tables S2-S3 report the rest of the matrices for the six  
384 sites, which show the same general relationships as those in Table 2. The crustal-derived species  
385 ( $\text{Ca}^{2+}$ ,  $\text{Mg}^{2+}$ ,  $\text{K}^+$ ,  $\text{Na}^+$ ,  $\text{Cl}^-$ ) exhibit statistically significant correlations (95% confidence using a  
386 two-tailed Student's T-Test; this condition applies to all correlations reported hereinafter) with  
387 each other in both rain and snow ( $r = 0.48 - 1.00$ ,  $n = 90 - 107$ ), suggesting that their common  
388 source is dust or sea salt depending on the site. Sodium and  $\text{Cl}^-$  are strongly correlated at the site  
389 closest to marine emissions, Organ Pipe ( $r = 1.00$ ). These two species exhibit high correlations  
390 for both rain and snow at the other sites too ( $r = 0.66 - 0.97$ ).

391  
392 Sulfate,  $\text{NH}_4^+$ , and  $\text{NO}_3^-$  are highly correlated with each other relative to other species in rain and  
393 snow reflecting non-crustal sources, specifically anthropogenic emissions in the form of  $\text{SO}_2$ ,  
394 nitrogen oxides ( $\text{NO}_x$ ), and ammonia ( $\text{NH}_3$ ). Sulfate,  $\text{NO}_3^-$ , and  $\text{NH}_4^+$  in precipitation originate  
395 from scavenging of these species in the aerosol phase and also from transfer of their vapor  
396 precursors:  $\text{SO}_4^{2-}$  from  $\text{SO}_2$ ;  $\text{NO}_3^-$  from nitric acid ( $\text{HNO}_3$ ), which originates from  $\text{NO}_x$   
397 emissions;  $\text{NH}_4^+$  from  $\text{NH}_3$ . Ammonium typically serves as a base for sulfuric and nitric acids  
398 and originates from  $\text{NH}_3$ , which is emitted from livestock waste, fertilizer applications, biomass  
399 burning, motor vehicle emissions, and coal combustion (e.g. Apsimon et al., 1987; Asman and  
400 Janssen, 1987; Kleeman et al., 1999; Anderson et al., 2003; Batty et al., 2003; Sorooshian et al.,  
401 2008). The dominant route by which  $\text{SO}_4^{2-}$  becomes associated with drops is thought to be  
402 aerosol scavenging (e.g. van der Swaluw et al., 2011). Other work has shown that the close  
403 relationship between  $\text{SO}_4^{2-}$  and  $\text{NO}_3^-$  in rain and snow is mainly linked to anthropogenic inputs  
404 (e.g. Wake et al., 1992; Legrand and Mayewski, 1997; Schwikowski et al., 1999; Preunkert et al.,  
405 2003; Olivier et al., 2006; Dias et al., 2012). Ammonia from anthropogenic sources has also been  
406 linked to soluble ion measurements in ice and rain (Kang et al., 2002; Hou et al., 2003).

407  
408 The crustal cation species ( $\text{Ca}^{2+}$ ,  $\text{Mg}^{2+}$ ,  $\text{K}^+$ ,  $\text{Na}^+$ ) exhibit statistically significant correlations with  
409  $\text{SO}_4^{2-}$ ,  $\text{NO}_3^-$ , and  $\text{Cl}^-$  at all sites. This is suggestive of reactions of acids (e.g. nitric, sulfuric,  
410 hydrochloric acids) with crustal surfaces such as dust and sea salt (e.g. Matsuki et al., 2010).  
411 This link is supported by a large inventory of previous work: (i) measurements in Asia indicate  
412 that dust is a significant source of  $\text{SO}_4^{2-}$ , largely of anthropogenic origin which comes together

413 with dust, in snow and glaciers (Wake et al., 1990; Kreutz et al., 2001; Zhao et al., 2011); (ii) a  
414 close association of  $\text{SO}_4^{2-}$  with crustal matter was argued to explain the close relationship  
415 between  $\text{SO}_4^{2-}$  and  $\text{Ca}^{2+}$  in rain water in India (Satyanarayana et al., 2010); (iii) Zhang et al.  
416 (2007) suggested that acids such as HCl react with windblown crustal particles to yield a high  
417  $\text{Mg}^{2+}/\text{Cl}^-$  correlation in China; and (iv) dust surfaces have been shown to become coated with  
418 soluble species such as  $\text{SO}_4^{2-}$ ,  $\text{NO}_3^-$ , and  $\text{Cl}^-$  (Desbouefs et al., 2001; Sullivan et al., 2007;  
419 Matsuki et al., 2010) leading to enhanced hygroscopic properties (Levin et al., 1996; Koehler et  
420 al., 2007; Crumeyrolle et al., 2008; Sorooshian et al., 2012). Correlations between similar subsets  
421 of species (crustal species,  $\text{SO}_4^{2-}/\text{NH}_4^+/\text{NO}_3^-$ , and the combination of the latter two) have also  
422 been observed in other regions such as the Mediterranean, Turkey, India, Brazil, Mexico, and  
423 China (Al-Momani et al., 1997; Basak and Agha, 2004; Safai et al., 2004; Mouli et al., 2005;  
424 Baez et al., 2007; Zhang et al., 2007; Teixeira et al., 2008; Yi et al., 2010; Raman and  
425 Ramachandran, 2011).

426

### 427 **5.1.2 Interrelationships between aerosol and precipitation species**

428

429 It is of interest to examine the extent to which aerosol and precipitation species concentrations  
430 are related. As  $\text{SO}_4^{2-}$  and fine soil represent the most abundant  $\text{PM}_{2.5}$  constituents of interest in  
431 this work (excluding other constituents such as carbonaceous species), their particulate  
432 concentrations are compared to all precipitation species concentrations in Table 3. The following  
433 factors could bias the interpretation of these results: (i) gases that partition to hydrometeors; and  
434 (ii) different air masses affecting altitudes at which the IMPROVE measurements take place and  
435 where precipitation is produced. With the exception of Organ Pipe, crustal-derived species in  
436 rain ( $\text{Ca}^{2+}$ ,  $\text{Mg}^{2+}$ ,  $\text{K}^+$ ,  $\text{Cl}^-$ ,  $\text{Na}^+$ ) exhibit statistically significant correlations with fine soil.  
437 Although not shown in Table 3, particulate  $\text{Cl}^-$  was only correlated with rain  $\text{Cl}^-$  ( $r = 0.29$ ;  $n =$   
438  $105$ ) at one site (Organ Pipe) because of the proximity of Organ Pipe to the Pacific Ocean;  
439 particulate  $\text{Cl}^-$  was also correlated with  $\text{Na}^+$  at this site ( $r = 0.29$ ,  $n = 105$ ). Interestingly,  $\text{NH}_4^+$ ,  
440  $\text{SO}_4^{2-}$ , and  $\text{NO}_3^-$  in rain are also correlated with fine soil at four sites including Organ Pipe. This  
441 result is consistent with these same anthropogenically-related species being related to the crustal  
442 species in the rain data. Fine soil levels exhibit statistically significant correlations with those of  
443 crustal-derived species in snow at Bryce Canyon, Mesa Verde, and Gila.

444

445 Particulate  $\text{SO}_4^{2-}$  exhibits a statistically significant correlation with  $\text{SO}_4^{2-}$  in rain at all sites  
446 except Chiricahua. Particulate  $\text{SO}_4^{2-}$  was also correlated with  $\text{NO}_3^-$  and  $\text{NH}_4^+$  in rain at four sites  
447 including Organ Pipe and Chiricahua. Particulate  $\text{SO}_4^{2-}$  exhibits few statistically significant  
448 correlations with snow species: it only exhibited positive correlations with  $\text{SO}_4^{2-}$  and  $\text{NO}_3^-$  at  
449 Bryce Canyon. The different relationships of particulate  $\text{SO}_4^{2-}$  with  $\text{SO}_4^{2-}$  in rain and snow may  
450 be caused by the vertical structure of  $\text{SO}_4^{2-}$  (and precursors) in the atmosphere and the varying  
451 degree to which  $\text{SO}_4^{2-}$ -enriched particles act as CCN versus IN in the region. Sulfate (and  
452 precursor) concentrations decrease with altitude since its sources are near the surface. It is noted  
453 that monthly-averaged particulate  $\text{SO}_4^{2-}$  concentrations generally decrease from the lowest-  
454 elevation IMPROVE stations to the highest ones (Fig. 6). Sulfate-rich particles are hygroscopic  
455 and expected to be efficient CCN, which likely are removed by warm rain prior to reaching  
456 higher freezing altitudes where IN activation occurs.

457

458 Motivated by previous findings that dust particles act as IN, the coarse:fine aerosol mass  
459 concentration ratio is compared to snow and rain chemical concentrations (Table 3). The  
460 coarse:fine ratio exhibited statistically insignificant correlations with most rain water species at  
461 all sites. However, the same ratio is positively correlated with snow species at all sites except  
462 Chiricahua and Organ Pipe, where the latter site experienced no snow. The coarse:fine ratio was  
463 typically only correlated with the crustal species ( $\text{Ca}^{2+}$ ,  $\text{Mg}^{2+}$ ,  $\text{Na}^+$ ,  $\text{K}^+$ ,  $\text{Cl}^-$ ) and  $\text{NO}_3^-$ , suggestive  
464 of a preferential role of coarse particles as IN in the region.  
465

## 466 5.2 Species influencing precipitation pH

467  
468 The six sites exhibit similar interrelationships between precipitation chemical concentrations and  
469 pH (Table 2 and Tables S2-S3). The crustal-derived rain and snow species ( $\text{Ca}^{2+}$ ,  $\text{Mg}^{2+}$ ,  $\text{Na}^+$ ,  $\text{K}^+$ )  
470 are positively correlated with pH. The  $\text{PM}_{2.5}$  aerosol constituents that rain and snow pH are best  
471 correlated with are Ca, K, Na, and fine soil (Table S4). These results provide support for dust  
472 increasing precipitation pH in the region, which is consistent with increases in the following  
473 parameters during the season with highest rain pH (i.e. MAMJ): fine soil and coarse aerosol  
474 concentrations, particulate crustal species concentrations (Ca, Mg, Na), the coarse:fine aerosol  
475 ratio, and UV AI. The MAMJ pH peak in the Southwest is in contrast to India, where the highest  
476 values are observed during the monsoon due to large inputs of sea salt from marine-derived air  
477 masses (Satyanarayana et al., 2010). Ammonium was also positively correlated with pH at three  
478 sites (Bryce Canyon, Bandelier, Chiricahua), albeit more weakly than other cations. The weaker  
479 relationship between pH and  $\text{NH}_4^+$  as compared to traditional crustal-derived bases such as  $\text{Ca}^{2+}$   
480 suggests that the latter are more effective regionally as neutralization agents; this has also been  
481 observed in other regions such as the Eastern Mediterranean and Turkey (e.g. Al-Momani et al.,  
482 1997; Basak and Alagha 2004). Sulfate is negatively correlated with snow (Bryce Canyon, Gila,  
483 Mesa Verde) and rain pH (Mesa Verde) because of its acidic nature. Sulfate is the main  
484 dominant source of acidity in precipitation in other regions such as Brazil (Teixiera et al., 2008).  
485

## 486 5.3 Nitrate:Sulfate ratio

487  
488 The precipitation  $\text{NO}_3^-:\text{SO}_4^{2-}$  ratios in this study, and those of Hutchings et al. (2009) in the same  
489 region, are higher than those observed in other regions. In this study, the cumulative average at  
490 each site ranges from 0.97 – 1.49 for rain and 0.74 - 2.08 for snow, using concentrations units of  
491  $\mu\text{eq L}^{-1}$ . These units are now applied for comparison with documented values in the following  
492 regions: Brazil (~ 1.10, Dias et al., 2012; ~ 0.61, Migliavacca et al., 2004; ~ 0.11, Migliavacca et  
493 al., 2005); Turkey (~ 0.625, Topcu et al., 2002); Jordan (~ 0.51, Al-Khashman, 2005); India (~  
494 0.28, Singh et al., 2007); Costa Rica (~ 0.05, Herrera et al., 2009); Spain (~ 0.46 from 1984 –  
495 1993 and ~ 0.94 from 1998 - 2009; Izquierdo et al., 2012); Mexico (~ 1.03; Baez et al., 2007);  
496 and numerous sites in Asia including in China, Japan, the Philippines, Thailand, Vietnam,  
497 Malaysia, and Hong Kong (~ 0.36 – 1.14, Yeung et al., 2007). The sites with the lowest ratios  
498 were strongly influenced by  $\text{SO}_2$  and source types such as vehicles, volcanoes, refineries,  
499 petrochemical activity, and thermoelectric plants. The  $\text{NO}_3^-:\text{SO}_4^{2-}$  ratio is hypothesized to be  
500 larger in the Southwest due to some combination of the following: (i) different time ranges of  
501 data collection, which would make the comparisons less meaningful due to varying levels of  
502 pollution regulations at different times and locations; (ii) reduced  $\text{SO}_2$  emissions as compared to  
503 the other regions; and (iii) enhanced  $\text{NO}_3^-$  either due to its association with crustal matter or

504 partitioning of its gaseous precursors into rain and snow. With regard to periods of data  
505 collection, it is critical to note that at least in North America, more significant reductions in SO<sub>2</sub>  
506 as compared to NO<sub>x</sub> over recent decades likely bias intercomparisons of NO<sub>3</sub><sup>-</sup>:SO<sub>4</sub><sup>2-</sup> ratios  
507 between different studies (e.g. EPA, 2003; Kvale and Pryor, 2006). Measurements in the eastern  
508 United States have pointed to reductions in precipitation sulfate unlike nitrate since the 1980s  
509 (e.g. Butler and Likens, 1991; Lynch et al., 1995; Nilles and Conley, 2001; Butler et al., 2001).

510  
511 The precipitation NO<sub>3</sub><sup>-</sup>:SO<sub>4</sub><sup>2-</sup> ratios in this study are also interesting in the following two ways:  
512 (i) they are higher in precipitation samples as compared to PM<sub>2.5</sub> (0.16 – 0.47); and (ii) the NO<sub>3</sub><sup>-</sup>  
513 :SO<sub>4</sub><sup>2-</sup> ratio in rain typically increases from DJF (0.64 – 1.16) until JAS (1.09 – 1.63) before  
514 decreasing again, which is the opposite temporal trend for the particulate NO<sub>3</sub><sup>-</sup>:SO<sub>4</sub><sup>2-</sup> ratio. One  
515 explanation for both findings could be that the coarse aerosol fraction has higher NO<sub>3</sub><sup>-</sup>:SO<sub>4</sub><sup>2-</sup>  
516 ratios than what is reported for PM<sub>2.5</sub>, and that those larger particles efficiently serve as CCN and  
517 IN thereby driving up the ratio in precipitation. To indirectly examine the potential role of coarse  
518 aerosol in influencing the precipitation ratios, the coarse:fine aerosol mass ratio was compared to  
519 the NO<sub>3</sub><sup>-</sup>:SO<sub>4</sub><sup>2-</sup> rain water ratio (Fig. S2). The two ratios do not exhibit a statistically significant  
520 positive relationship, and the coarse:fine ratio is typically the smallest in JAS. This weakens the  
521 case for nucleation scavenging of coarse particles with high NO<sub>3</sub><sup>-</sup>:SO<sub>4</sub><sup>2-</sup> ratios, assuming that the  
522 air masses affecting clouds are similar to those influencing the IMPROVE stations. Another  
523 potential explanation is that gaseous precursors of NO<sub>3</sub><sup>-</sup> are scavenged more effectively in clouds  
524 relative to those for SO<sub>4</sub><sup>2-</sup>. Hayden et al. (2008) used airborne measurements to show that the  
525 NO<sub>3</sub><sup>-</sup>:SO<sub>4</sub><sup>2-</sup> ratio usually was higher in cloud drop residual particles than sub-cloud particles, and  
526 that the predominant mechanism by which NO<sub>3</sub><sup>-</sup> partitioned to drops was by transfer of gas-phase  
527 HNO<sub>3</sub>. That study showed that unlike NO<sub>3</sub><sup>-</sup>, SO<sub>4</sub><sup>2-</sup> partitioned to drops mainly by nucleation  
528 scavenging. Independent measurements on a mountaintop in Sweden showed that NO<sub>3</sub><sup>-</sup> activated  
529 more efficiently than SO<sub>4</sub><sup>2-</sup> into cloud drops (Drewnick et al., 2007). However, our results show  
530 that particulate NO<sub>3</sub><sup>-</sup> concentrations only exhibit a statistically significant correlation with  
531 precipitation NO<sub>3</sub><sup>-</sup> levels at one of the six sites (Gila: r = 0.34, n = 265), whereas SO<sub>4</sub><sup>2-</sup> shows a  
532 positive relationship between rain and aerosol at five of the six sites. Therefore, the preferential  
533 activation of NO<sub>3</sub><sup>-</sup> rather than SO<sub>4</sub><sup>2-</sup> is ruled out here as the explanation. A more plausible  
534 explanation could be the efficient transfer of gaseous precursors of NO<sub>3</sub><sup>-</sup> to rain and snow, which  
535 cannot be quantified with surface aerosol measurements. The annual cycle of HNO<sub>3</sub> at a site in  
536 the Southwest (Johnson et al., 1994) was previously measured to be the same as NO<sub>3</sub><sup>-</sup>:SO<sub>4</sub><sup>2-</sup> in  
537 our study, which can help explain the increase of this ratio in rain from the wintertime to JAS.

538  
539 Another interesting observation in the Southwest is that the NO<sub>3</sub><sup>-</sup> mass fraction and the NO<sub>3</sub><sup>-</sup>  
540 :SO<sub>4</sub><sup>2-</sup> ratio are both higher in snow relative to rain during DJF. In contrast, NH<sub>4</sub><sup>+</sup> and SO<sub>4</sub><sup>2-</sup> both  
541 exhibit higher overall mass fractions in rain relative to snow during DJF. One explanation is the  
542 efficient adsorption of gaseous NO<sub>3</sub><sup>-</sup> precursors such as HNO<sub>3</sub> to snow (e.g. Jacobi et al., 2012);  
543 however, the relative strength of partitioning of HNO<sub>3</sub> to rain drops and snow is uncertain and  
544 requires additional investigation for this region. Another explanation could be the preferential  
545 role of different particle types in serving as CCN versus IN, which was already suggested to  
546 explain why particulate SO<sub>4</sub><sup>2-</sup> was mainly correlated with SO<sub>4</sub><sup>2-</sup> in rain rather than snow. More  
547 effective nucleation scavenging of hygroscopic particles containing SO<sub>4</sub><sup>2-</sup> at lower altitudes in  
548 the form of CCN would limit their ability to reach higher altitudes where deeper clouds produce  
549 snow. At those higher altitudes, dust particles can serve as effective IN (Isono and Ikebe, 1960;

550 Kumai, 1961; Twohy and Gandrud, 1998; Heintzenberg et al., 1996; DeMott et al., 2003a/b;  
551 Sassen et al., 2003; Czizco et al., 2004; Koehler et al., 2007; Prenni et al., 2007; Zimmermann et  
552 al., 2008), and as noted already, they contain enhanced levels of  $\text{NO}_3^-$  due to reactions with  
553  $\text{HNO}_3$  (e.g. Malm et al., 2004; Lee et al., 2008). This speculation is partly supported by the  
554 finding that the coarse:fine aerosol ratio was positively correlated with snow pH at more sites  
555 (Bryce Canyon, Gila, Mesa Verde) than with rain pH (Mesa Verde). But a conflicting result is  
556 that the snow ratio of  $\text{NO}_3^-:\text{SO}_4^{2-}$  does not exhibit a statistically significant relationship with the  
557 coarse:fine aerosol mass ratio at any site. It is unclear as to whether this is due to dissimilar air  
558 masses influencing altitudes where snow is produced relative to the IMPROVE stations. More  
559 detailed investigations would assist with explaining the findings above related to the  $\text{NO}_3^-:\text{SO}_4^{2-}$   
560 ratios, especially examining  $\text{HNO}_3$  partitioning behavior and the role of different particle types in  
561 serving as CCN and IN in the Southwest.

562

#### 563 **5.4 Interannual variability in aerosol and precipitation chemistry**

564

565 Previous analyses of NADP/NTN concentration data over the United States between 1985 and  
566 2002 showed general increases in ammonium, reductions in sulfate, and mixed changes in nitrate  
567 depending on location (Lehmann et al., 2005); furthermore, reductions in sulfate have been  
568 shown to be more significant as compared to nitrate (Lehmann et al., 2011). As JAS is the season  
569 with the most available precipitation data across all sites, a long-term trend analysis for this  
570 season shows that the only species in rain exhibiting a statistically significant concentration  
571 change is  $\text{SO}_4^{2-}$  (Table 4). This species exhibited a decreasing trend at Bryce Canyon ( $-0.062 \text{ mg}$   
572  $\text{L}^{-1} \text{ y}^{-1}$ ) and Gila Cliff ( $-0.057 \text{ mg L}^{-1} \text{ y}^{-1}$ ). The decreasing trend is ubiquitous across the region in  
573 the fine aerosol fraction, with the largest reduction at Organ Pipe ( $-0.109 \mu\text{g m}^{-3} \text{ y}^{-1}$ ); the  
574 reduction at other sites ranged between  $-0.029$  and  $-0.047 \mu\text{g m}^{-3} \text{ y}^{-1}$ . This reduction in the region  
575 can be explained by air regulations of  $\text{SO}_4^{2-}$  precursors (e.g. Matichuk et al., 2006; Sorooshian et  
576 al., 2011). Nitrate does not exhibit a statistically significant change in concentration in rain or in  
577 particles, except relatively small reductions as compared to  $\text{SO}_4^{2-}$  at Chiricahua ( $-0.006 \mu\text{g m}^{-3} \text{ y}^{-1}$ )  
578 and Organ Pipe ( $-0.016 \mu\text{g m}^{-3} \text{ y}^{-1}$ ). Other work in the Southwest has suggested that a lack of a  
579 change of  $\text{NO}_3^-$  over the last decade in at least one part of the Southwest (i.e. southern Arizona)  
580 may be due to competing factors: (i) land-use changes (e.g. agricultural land to urban areas) can  
581 reduce  $\text{NH}_3$  emissions and particulate  $\text{NO}_3^-$  formation; and (ii) higher  $\text{NO}_x$  emissions linked to  
582 population growth and reductions in  $\text{SO}_4^{2-}$  allow for more  $\text{NH}_3$  to neutralize  $\text{HNO}_3$  to promote  
583 ammonium nitrate ( $\text{NH}_4\text{NO}_3$ ) production (Sorooshian et al., 2011). While the  $\text{NO}_3^-:\text{SO}_4^{2-}$  ratio in  
584 the fine aerosol fraction only increased at one site (Mesa Verde), there was an increase in rain at  
585 all sites except Chiricahua and Organ Pipe. Rain pH has also increased at all sites except Mesa  
586 Verde and Organ Pipe; the increase at four of the sites is due to reductions in  $\text{SO}_4^{2-}$  as compared  
587 to increases in  $\text{NO}_3^-$ . A potential reason as to why Organ Pipe does not show increases in either  
588 the  $\text{NO}_3^-:\text{SO}_4^{2-}$  ratio or pH, even though it showed the largest reduction in particulate  $\text{SO}_4^{2-}$ , may  
589 be due to an increasingly important role for coarse particle types relative to fine particles. More  
590 specifically, Organ Pipe was the only site to show an increase in the coarse:fine aerosol mass  
591 ratio in JAS, with an increasing rate of  $0.084 \text{ y}^{-1}$ . This result is suggestive of the presence of  
592 more coarse particle types, mainly sea salt and dust, that can react with  $\text{HNO}_3$  to form particulate  
593  $\text{NO}_3^-$ , simultaneous with reduced fine aerosol  $\text{SO}_4^{2-}$  over time.

594

#### 595 **6 Conclusions**

596

597 This study characterized aerosol and precipitation composition at six sites in the US Southwest.  
598 The main results of this work are as follows, following the order of questions posed in Section 1:

599

600 (i) Precipitation accumulation is concentrated in a wintertime mode (DJF) and a monsoon mode  
601 (JAS), with only warm rain associated with the latter. The relative amount of rain and snow  
602 during DJF depends on geography and altitude, with rain being more abundant farther south near  
603 the international border and at lower altitudes. All aerosol and precipitation species  
604 concentrations typically were highest during MAMJ (including precipitation pH) due to  
605 increased dust concentrations.

606

607 (ii) Statistically significant relationships in the regional rain and snow are observed for numerous  
608 crustal-derived species ( $\text{Ca}^{2+}$ ,  $\text{Mg}^{2+}$ ,  $\text{K}^+$ ,  $\text{Na}^+$ ), mainly from dust, and a subset of species with  
609 anthropogenic sources ( $\text{NH}_4^+$ ,  $\text{SO}_4^{2-}$ ,  $\text{NO}_3^-$ ). Species in the crustal group also exhibit positive  
610 relationships with  $\text{SO}_4^{2-}$ ,  $\text{NO}_3^-$ , and  $\text{Cl}^-$ , suggesting that acidic gases likely react with and  
611 partition to either coarse crustal particles or hydrometeors enriched with crustal constituents.  
612 Organ Pipe, the site closest to the Pacific Ocean, shows an especially strong relationship between  
613  $\text{Na}^+$  and  $\text{Cl}^-$  in rain water due to sea salt influence, indicating that this aerosol type more strongly  
614 affects precipitation in parts of the Southwest closest to the ocean.

615

616 (iii) Rain and snow pH levels were usually between 5 – 6. Rain pH was highest during MAMJ,  
617 which was coincident with the highest rain and particulate concentrations of crustal-derived  
618 species ( $\text{Ca}^{2+}$ ,  $\text{Mg}^{2+}$ ,  $\text{K}^+$ ,  $\text{Na}^+$ ). Rain and snow pH were generally well-correlated with these  
619 species showing that dust in the region is highly influential in acid-neutralization.

620

621 (iv) Crustal-derived species in both rain and snow ( $\text{Ca}^{2+}$ ,  $\text{Mg}^{2+}$ ,  $\text{K}^+$ ,  $\text{Cl}^-$ ,  $\text{Na}^+$ ) exhibit statistically  
622 significant correlations with particulate fine soil. The coarse: fine aerosol mass ratio was  
623 correlated with snow concentrations of crustal species ( $\text{Ca}^{2+}$ ,  $\text{Mg}^{2+}$ ,  $\text{Na}^+$ ,  $\text{K}^+$ ,  $\text{Cl}^-$ ) and  $\text{NO}_3^-$ ,  
624 suggestive of a preferential role of coarse particles (mainly dust) as IN in the region. Particulate  
625  $\text{SO}_4^{2-}$  concentrations exhibit a statistically significant correlation with rain  $\text{SO}_4^{2-}$  at most sites  
626 unlike snow, which may be related to a combination of the vertical structure of  $\text{SO}_4^{2-}$  (and  
627 precursors) in the atmosphere and the varying degree to which  $\text{SO}_4^{2-}$ -enriched particles act as  
628 CCN versus IN in the region.

629

630 (v) The precipitation  $\text{NO}_3^-:\text{SO}_4^{2-}$  ratios in this study exhibit the following features: (i) higher in  
631 precipitation samples as compared to  $\text{PM}_{2.5}$ ; (ii) exhibit the opposite annual cycle compared to  
632 the particulate  $\text{NO}_3^-:\text{SO}_4^{2-}$  ratio; and (iii) are higher in snow relative to rain during DJF. Multiple  
633 explanations are discussed that require more detailed investigation, including partitioning of  
634 gaseous  $\text{NO}_3^-$  precursors (i.e.  $\text{HNO}_3$ ) to rain and snow.

635

636 (vi) Long-term trend analysis for rain chemistry during the monsoon season (JAS) shows that the  
637  $\text{NO}_3^-:\text{SO}_4^{2-}$  ratio increased at most sites, due to air regulations reducing  $\text{SO}_4^{2-}$  precursor  
638 concentrations. Sulfate was the particulate species showing the most consistent reduction over  
639 time across the Southwest. The only site that did not exhibit an increase in either the  $\text{NO}_3^-:\text{SO}_4^{2-}$   
640 ratio or pH in rain was Organ Pipe, which exhibited the only long-term increase in the particulate  
641 coarse: fine mass ratio. Increasing relative amounts of coarse particles as compared to fine

642 particles is thought to increase rain pH due to reduced influence from fine particulate  $\text{SO}_4^{2-}$  and  
643 increased influence from basic particulate species that are concentrated in the coarse fraction.  
644 Furthermore, reactions of  $\text{HNO}_3$  with coarse particle types and potential partitioning of this  
645 species to rain and snow can promote higher  $\text{NO}_3^-:\text{SO}_4^{2-}$  ratios.

646  
647 Future research is needed to test hypotheses used in this work to explain some of the results for  
648 the Southwest, including (i) the role of different particle types in serving as CCN and IN and (ii)  
649 the partitioning behavior of gases such as  $\text{HNO}_3$  to particles and hydrometeors. While this work  
650 has looked at factors influencing precipitation chemistry, it is noted that another major issue in  
651 the Southwest is deposition of aerosol particles to high altitude areas that reside in the snowpack  
652 or fall as summer rain and release nutrients into downstream ecosystems (Psenner, 1999;  
653 Lawrence and Neff, 2009). For example, mineral dust is thought to be among the strongest  
654 sources of atmospheric phosphorus (Okin et al., 2004; Mahowald et al., 2008) and its deposition  
655 at high-elevation sites represents a major nutrient source for lakes (Morales-Baquero et al., 2006;  
656 Vicars and Sickman, 2011). Case studies in the Southwest have shown that dust events can  
657 influence the composition of snow water, specifically leading to enhancements in snowpack pH  
658 and calcium levels (Rhoades et al., 2010). Similar findings have linked dust to elemental  
659 composition of both precipitation and snow and changes in surface water chemistry (e.g. Landers  
660 et al., 1987; Turk et al., 2001). Other work has suggested that aerosol deposition can be a source  
661 of harmful contaminants such as lead (Liptzin and Seastedt, 2010).

662  
663 Dust particles can also have a large impact on the melt rate of mountain snowpacks in Colorado  
664 by lowering the albedo, from 0.7 to 0.4 on average, and thereby increasing shortwave radiation  
665 inputs to the snowpack (Painter et al., 2010; Skiles et al., 2012). We observed the highest coarse  
666 aerosol mass concentrations and other proxies of dust during MAMJ when snow is on the ground  
667 at most of the mountains surrounding the study sites. Recent work from Colorado has shown  
668 that the advancement in the loss of snow cover from dust, due to faster melts, is lineally related  
669 to the amount of dust in the snowpack, despite variability in irradiance and the timing of dust  
670 deposition (Skiles et al., 2012). Predicting the amounts of wet and dry dust deposition to and  
671 from the Southwest is therefore critical to predicting snowmelt rates and downstream water  
672 resources of the Colorado River Basin (Painter et al., 2010). More research is necessary to  
673 combine information on dust sources and deposition, as done in the current study, with regional  
674 variability in hydroclimate and snow processes (Harpold et al., 2012) in the mountains of the  
675 western US.

## 676 677 **Acknowledgements**

678 This research was supported by the Technology and Research Initiative Fund (TRIF),  
679 administered by the Arizona Board of Regents through the University of Arizona Water,  
680 Environmental, and Energy Solutions (WEES) initiative. Support was also provided by Grant 2  
681 P42 ES04940-11 from the National Institute of Environmental Health Sciences (NIEHS)  
682 Superfund Research Program, NIH. The authors gratefully acknowledge the NOAA Air  
683 Resources Laboratory (ARL) for the provision of the HYSPLIT transport and dispersion model  
684 and READY website (<http://ready.arl.noaa.gov>) used in this publication. The authors also  
685 acknowledge IMPROVE, NADP, and the Illinois State Water Survey for providing data. Some  
686 of the analyses and visualizations used in this study were produced with the Giovanni online data  
687 system, developed and maintained by the NASA GES DISC.

688

689 **References**

690 Adams, D. K., and Comrie, A. C.: The North American monsoon, *B. Am. Meteorol. Soc.*, 78,  
691 2197-2213, 1997.

692

693 Aherne, J., Mongeon, A., and Watmough, S. A.: Temporal and spatial trends in precipitation  
694 chemistry in the Georgia Basin, British Columbia, *J. Limnol.*, 69, 4-10, doi:10.3274/JI10-69-S1-  
695 02, 2010.

696

697 Al-Khashman, O. A.: Study of chemical composition in wet atmospheric precipitation in  
698 Eshidiya area, Jordan, *Atmos. Environ.*, 39, 6175-6183, 2005.

699

700 Al-Khashman, O. A.: Chemical characteristics of rainwater collected at a western site of Jordan,  
701 *Atmos. Res.*, 91, 53-61, 2009.

702

703 Al-Momani, I. F., Gullu, G., Olmez, I., Eler, U., Ortel, E., Sirin, G., and Tuncel, G.: Chemical  
704 composition of Eastern Mediterranean aerosol and precipitation: Indications of long-range  
705 transport, *Pure Appl. Chem.*, 69, 41-46, 1997.

706

707 Ames, R. B., and Malm, W. C.: Comparison of sulfate and nitrate particle mass concentrations  
708 measured by IMPROVE and the CDN, *Atmos. Environ.*, 35, (5), 905-916, 2001.

709

710 Anderson, N., Strader, R., and Davidson, C.: Airborne reduced nitrogen: ammonia emissions  
711 from agriculture and other sources, *Environ. Int.*, 29, 277-286, 2003.

712

713 Apsimon, H. M., Kruse, M., and Bell, J. N. B.: Ammonia emissions and their role in acid  
714 deposition, *Atmos. Environ.*, 21, 1939-1946, 1987.

715

716 Asman, W. A. H. and Janssen, A. J.: A long-range transport model for ammonia and ammonium  
717 for Europe, *Atmos. Environ.*, 21, 2099-2119, 1987.

718

719 Avila, A., Queralt-Mitjans, I., and Alarcón, M.: Minerological composition of Africa dust  
720 delivered by red rains over northeastern Spain, *J. Geophys. Res.*, 102(D18), 21977-21996, 1997.

721

722 Avila, A., Alarcón, M., and Queralt-Mitjans, I.: The chemical composition of dust transported in  
723 red rains-Its contribution to the biogeochemical cycle of a holm oak forest in Catalonia (Spain),  
724 *Atmos. Environ.*, 32, 179-191, 1998.

725

726 Baez, A., Belmont, R., Garcia, R., Padilla, H., and Torres, M. C.: Chemical composition of  
727 rainwater collected at a southwest site of Mexico City, Mexico, *Atmos. Res.*, 86, 61-75, 2007.

728

729 Balasubramanian, R., Victor, T., and Chun, N.: Chemical and statistical analysis of precipitation  
730 in Singapore, *Water Air Soil Poll.*, 130, 451-456, 2001.

731

732 Baron, J. S., Rueth, H. M., Wolfe, A. M., Nydick, K. R., Allstott, E. J., Minear, J. T., and  
733 Moraska, B.: Ecosystem responses to nitrogen deposition in the Colorado Front Range,  
734 Ecosystems, 3, 352-368, 2000.  
735  
736 Basak, B., and Alagha, O.: The chemical composition of rainwater over Buyukcekmece Lake,  
737 Istanbul, Atmos. Res., 71, 275-288, 2004.  
738  
739 Battye, W., Aneja, V. P., and Roelle, P. A.: Evaluation and improvement of ammonia emissions  
740 inventories, Atmos. Environ., 37, 3873–3883, 2003.  
741  
742 Bench, G., Fallon, S., Schichtel, B., Malm, W., and McDade, C.: Relative contributions of fossil  
743 and contemporary carbon sources to PM<sub>2.5</sub> aerosols at nine Interagency Monitoring for  
744 Protection of Visual Environments (IMPROVE) network sites, J. Geophys. Res., 112, D10205,  
745 doi:10.1029/2006jd007708, 2007.  
746  
747 Butler, T. J., and Likens, G. E.: The impact of changing regional emissions on precipitation  
748 chemistry in the eastern United-States, Atmos. Environ., 25, 305-315, doi:10.1016/0960-  
749 1686(91)90302-N, 1991.  
750  
751 Butler, T. J., Likens, G. E., and Stunder, B. J. B.: Regional-scale impacts of Phase I of the Clean  
752 Air Act Amendments in the USA: the relation between emissions and concentrations, both wet  
753 and dry, Atmos. Environ., 35, 1015-1028, doi:10.1016/S1352-2310(00)00386-1, 2001.  
754  
755 Butler, T. J., Likens, G. E., Vermeylen, F. M., and Stunder, B. J. B.: The relation between NO<sub>x</sub>  
756 emissions and precipitation NO<sub>3</sub><sup>-</sup> in the eastern USA, Atmos. Environ., 37, 2093-2104,  
757 doi:10.1016/S1352-2310(03)00103-1, 2003.  
758  
759 Cahill, T. M.: Annual cycle of size-resolved organic aerosol characterization in an urbanized  
760 desert environment, Atmos. Environ., 71, 226-233, doi:10.1016/j.atmosenv.2013.02.004, 2013.  
761  
762 Cayan, D. R., Das, T., Pierce, D. W., Barnett, T. P., Tyree, M., and Gershunov, A.: Future  
763 dryness in the southwest US and the hydrology of the early 21st century drought, P. Natl. Acad.  
764 Sci. USA, 107, 21271-21276, doi:10.1073/pnas.0912391107, 2010.  
765  
766 Collett, J. L., Bator, A., Sherman, D. E., Moore, K. F., Hoag, K. J., Demoz, B. B., Rao, X., and  
767 Reilly, J. E.: The chemical composition of fogs and intercepted clouds in the United States,  
768 Atmos. Res., 64, 29-40, doi:10.1016/S0169-8095(02)00077-7, 2002.  
769  
770 Crumeyrolle, S., Gomes, L., Tulet, P., Matsuki, A., Schwarzenboeck, A., and Crahan, K.:  
771 Increase of the aerosol hygroscopicity by cloud processing in a mesoscale convective system: a  
772 case study from the AMMA campaign, Atmos. Chem. Phys., 8, 6907–6924, doi:10.5194/acp-8-  
773 6907-2008, 2008.  
774  
775 Csavina, J., Field, J., Taylor, M. P., Gao, S., Landazuri, A., Betterton, E. A., and Saez, A. E.: A  
776 review on the importance of metals and metalloids in atmospheric dust and aerosol from mining  
777 operations, Sci. Total Environ., 433, 58-73, 2012.

778 Cziczo, D. J., Murphy, D. M., Hudson, P. K., and Thomson, D. S.: Single particle measurements  
779 of the chemical composition of cirrus ice residue during CRYSTAL-FACE, *J. Geophys. Res.*,  
780 109, D04201, doi:10.1029/2003jd004032, 2004.  
781

782 DeMott, P. J., Sassen, K., Poellot, M. R., Baumgardner, D., Rogers, D. C., Brooks, S. D., Prenni,  
783 A. J., and Kreidenweis, S. M.: African dust aerosols as atmospheric ice nuclei, *Geophys. Res.*  
784 *Lett.*, 30, 1732, doi:10.1029/2003gl017410, 2003a.  
785

786 DeMott, P. J., Cziczo, D. J., Prenni, A. J., Murphy, D. M., Kreidenweis, S. M., Thomson, D. S.,  
787 Borys, R., and Rogers, D. C.: Measurements of the concentration and composition of nuclei for  
788 cirrus formation, *P. Natl. Acad. Sci. USA*, 100, 14655-14660, doi:10.1073/pnas.2532677100,  
789 2003b.  
790

791 Desboeufs, K. V., Losno, R., and Colin, J. L.: Factors influencing aerosol solubility during cloud  
792 processes, *Atmos. Environ.*, 35, 3529–3537, 2001.  
793

794 Dias, V. R. D., Sanches, L., Alves, M. D., and Nogueira, J. D.: Spatio-temporal variability of  
795 anions in wet precipitation of Cuiaba, Brazil, *Atmos. Res.*, 107, 9-19, 2012.  
796

797 Draxler, R. R. and Rolph, G. D.: HYSPLIT (HYbrid Single-Particle Lagrangian Integrated  
798 Trajectory) Model access via NOAA ARL  
799 READY Website (<http://ready.arl.noaa.gov/HYSPLIT.php>); NOAA Air Resources Laboratory:  
800 Silver Spring, MD, 2012.  
801

802 Drewnick, F., Schneider, J., Hings, S. S., Hock, N., Noone, K., Targino, A., Weimer, S., and  
803 Borrmann, S.: Measurement of ambient, interstitial, and residual aerosol particles on a  
804 mountaintop site in central Sweden using an aerosol mass spectrometer and a CVI, *J. Atmos.*  
805 *Chem.*, 56, 1-20, 2007.  
806

807 EANET: Second Periodic Report on the State of Acid Deposition in East Asia, Part III Executive  
808 Summary, Acid Deposition Monitoring Network in East Asia, <http://www.eanet.asia/product/>,  
809 2011.  
810

811 Environmental Protection Agency: Latest Findings on National Air Quality: 2002 Status and  
812 Trends. Office of Air Quality and Standards, Air Quality Strategies and Standards Division,  
813 Research Triangle Park, NC., 2003.  
814

815 Fenn, M. E., Poth, M. A., Aber, J. D., Baron, J. S., Bormann, B. T., Johnson, D. W., Lemly, A.  
816 D., McNulty, S. G., Ryan, D. E., and Stottlemeyer, R.: Nitrogen excess in North American  
817 ecosystems: Predisposing factors, ecosystem responses, and management strategies, *Ecol. Appl.*,  
818 8, 706-733, 1998.  
819

820 Fenn, M. E., Baron, J. S., Allen, E. B., Rueth, H. M., Nydick, K. R., Geiser, L., Bowman, W. D.,  
821 Sickman, J. O., Meixner, T., Johnson, D. W., and Neitlich, P.: Ecological effects of nitrogen  
822 deposition in the western United States, *Bioscience*, 53, 404-420, 2003.  
823

824 Fernandez, D. P., Neff, J. C., and Reynolds, R. L.: Biogeochemical and ecological impacts of  
825 livestock grazing in semi-arid southeastern Utah, USA, *J. Arid. Environ.*, 72, 777-791, 2008.  
826  
827 Galy-Lacaux, C., Laouali, D., Descroix, L., Gobron, N., and Lioussé, C.: Long term precipitation  
828 chemistry and wet deposition in a remote dry savanna site in Africa (Niger), *Atmos. Chem.*  
829 *Phys.*, 9, 1579-1595, 2009.  
830  
831 Granat, L., Suksomsankh, K., Simachaya, S., Tabucanon, M., and Rodhe, R.: Regional  
832 background acidity and chemical composition of precipitation in Thailand, *Atmos. Environ.*, 30,  
833 1589-1596, 1996.  
834  
835 Harpold, A., Brooks, P., Rajagopal, S., Heidebuchel, I., Jardine, A., and Stielstra, C.: Changes in  
836 snowpack accumulation and ablation in the intermountain west, *Water Resour. Res.*, 48,  
837 W11501, doi:10.1029/2012wr011949, 2012.  
838  
839 Hayden, K. L., Macdonald, A. M., Gong, W., Toom-Saunty, D., Anlauf, K. G., Leithead, A., Li,  
840 S. M., Leitch, W. R., and Noone, K.: Cloud processing of nitrate, *J. Geophys. Res.*, 113,  
841 D18201, doi:10.1029/2007jd009732, 2008.  
842  
843 Heintzenberg, J., Okada, K., and Strom, J.: On the composition of non-volatile material in upper  
844 tropospheric aerosols and cirrus crystals, *Atmos. Res.*, 41, 81-88, 1996.  
845  
846 Herrera, J., Rodriguez, S., and Baez, A. P.: Chemical composition of bulk precipitation in the  
847 metropolitan area of Costa Rica, Central America, *Atmos. Res.*, 94, 151-160, 2009.  
848  
849 Herut, B., Starinsky, A., Katz, A., and Rosenfeld, D.: Relationship between the acidity and  
850 chemical composition of rainwater and climatological conditions along a transition zone between  
851 large deserts and Mediterranean climate, Israel, *Atmos. Environ.*, 34, 1281-1292, 2000.  
852  
853 Higgins, R. W., Yao, Y., and Wang, X. L.: Influence of the North American monsoon system on  
854 the US summer precipitation regime, *J. Climate*, 10, 2600-2622, 1997.  
855  
856 Hou, S. G., Qin, D. H., Zhang, D. Q., Kang, S. C., Mayewski, P. A., and Wake, C. P.: A 154a  
857 high-resolution ammonium record from the Rongbuk Glacier, north slope of Mt. Qomolangma  
858 (Everest), Tibet-Himal region, *Atmos. Environ.*, 37, 721-729, 2003.  
859  
860 Hsu, N. C., Herman, J. R., Torres, O., Holben, B. N., Tanre, D., Eck, T. F., Smirnov, A.,  
861 Chatenet, B., and Lavenu, F.: Comparisons of the TOMS aerosol index with Sun-photometer  
862 aerosol optical thickness: Results and applications, *J. Geophys. Res.*, 104, 6269-6279,  
863 doi:10.1029/1998jd200086, 1999.  
864  
865 Hutchings, J. W., Robinson, M. S., McIlwraith, H., Kingston, J. T., and Herckes, P.: The  
866 chemistry of intercepted clouds in northern Arizona during the North American Monsoon  
867 Season, *Water Air Soil Poll.*, 199, 191-202, 2009.  
868

869 Isono, K., and Ikebe, Y.: On the ice-nucleating ability of rock-forming minerals and soil  
870 particles, *J. Meteorol. Soc. Jpn.*, 38, 213–230, 1960.  
871

872 Izquierdo, R., Avila, A., and Alarcon, M.: Trajectory statistical analysis of atmospheric transport  
873 patterns and trends in precipitation chemistry of a rural site in NE Spain in 1984-2009, *Atmos.*  
874 *Environ.*, 61, 400-408, doi:10.1016/j.atmosenv.2012.07.060, 2012.  
875

876 Jacobi, H. W., Voisin, D., Jaffrezo, J. L., Cozic, J., and Douglas, T. A.: Chemical composition of  
877 the snowpack during the OASIS spring campaign 2009 at Barrow, Alaska, *J. Geophys. Res.*,  
878 117, D00r13, doi:10.1029/2011jd016654, 2012.  
879

880 Jaffe, D., Snow, J., and Cooper, O.: The 2001 Asian dust events: Transport and impact on  
881 surface aerosol concentrations in the U.S., *EOS Trans. AGU*, 84, 501–516, 2003.  
882

883 Johnson, B. J., Huang, S. C., Lecave, M., and Porterfield, M.: Seasonal trends of nitric-acid,  
884 particulate nitrate, and particulate sulfate concentrations at a southwestern United-States  
885 mountain site, *Atmos. Environ.*, 28, 1175-1179, 1994.  
886

887 Kang, S. C., Mayewski, P. A., Qin, D. H., Yan, Y. P., Zhang, D. Q., Hou, S. G., and Ren, J. W.:  
888 Twentieth century increase of atmospheric ammonia recorded in Mount Everest ice core, *J.*  
889 *Geophys. Res.*, 107, 4595, doi:10.1029/2001jd001413, 2002.  
890

891 Kavouras, I. G., Etyemezian, V., DuBois, D. W., Xu, J., and Pitchford, M.: Source reconciliation  
892 of atmospheric dust causing visibility impairment in Class I areas of the western United States, *J.*  
893 *Geophys. Res.*, 114, D02308, doi:10.1029/2008jd009923, 2009.  
894

895 Khemani, L. T., Momin, G. A., Naik, M. S., Rao, P. S. P., Safai, P. D., and Murty, A. S. R.:  
896 Influence of alkaline particulates on ph of cloud and rain water in India, *Atmos. Environ.*, 21,  
897 1137-1145, 1987.  
898

899 Kleeman, M. J., Hughes, L. S., Allen, J. O., and Cass, G. R.: Source contributions to the size and  
900 composition distribution of atmospheric particles: Southern California in September 1996,  
901 *Environ. Sci. Technol.*, 33, 4331–4341, 1999.  
902

903 Koehler, K. A., Kreidenweis, S. M., DeMott, P. J., Prenni, A. J., and Petters, M. D.: Potential  
904 impact of Owens (dry) Lake dust on warm and cold cloud formation, *J. Geophys. Res.*, 112,  
905 D12210, doi:10.1029/2007jd008413, 2007.  
906

907 Kreutz, K. J., Aizen, V. B., Cecil, L. D., and Wake, C. P.: Oxygen isotopic and soluble ionic  
908 composition of a shallow firn core, Inilchek glacier, central Tien Shan, *J. Glaciol.*, 47, 548-554,  
909 2001.  
910

911 Kulshrestha, U. C., Granat, L., Engardt, M., and Rodhe, H.: Review of precipitation monitoring  
912 studies in India-a search for region patterns, *Atmos. Environ.*, 39, 7403–7419, 2005.  
913

914 Kumai, M.: Snow crystals and the identification of the nuclei in the northern United-States of  
915 America, *J. Meteorol.*, 18, 139-150, 1961.

916

917 Kvale, K. F., and Pryor, S. C.: Precipitation composition in the Ohio River Valley: Spatial  
918 variability and temporal trends, *Water Air Soil Poll.*, 170, 143-160, doi:10.1007/s11270-006-  
919 2861-1, 2006.

920

921 Landers, D. H., Eilers, J. M., Brakke, D. F., Overton, W. S., Kellar, P. E., Silverstein, M. E.,  
922 Schonbrod, M. E., Crowe, R. D., Linthurst, R. E., Omernik, J. M., Teague, S. A., and Meier, E.  
923 P.: Western Lake Survey Phase I, characteristics of lakes in the western United States, Volume I:  
924 population description and physico-chemical relationships. Washington, D.C.: U.S.  
925 Environmental Protection Agency, EPA/600/3-86/054a, 176 pp, 1987.

926

927 Lawrence, C. R., and Neff, J. C.: The contemporary physical and chemical flux of aeolian dust:  
928 A synthesis of direct measurements of dust deposition, *Chem. Geol.*, 267, 46-63, 2009.

929

930 Lee, T., Kreidenweis, S. M., and Collett, J. L.: Aerosol ion characteristics during the Big Bend  
931 Regional Aerosol and Visibility Observational Study, *J. Air Waste Manage.*, 54, 585-592, 2004.

932

933 Lee, T., Yu, X. Y., Ayres, B., Kreidenweis, S. M., Malm, W. C., and Collett, J. L.: Observations  
934 of fine and coarse particle nitrate at several rural locations in the United States, *Atmos. Environ.*,  
935 42, 2720-2732, 2008.

936

937 Legrand, M., and Mayewski, P.: Glaciochemistry of polar ice cores: A review, *Rev. Geophys.*,  
938 35, 219-243, 1997.

939

940 Lehmann, C. M. B., Bowersox, V. C., and Larson, S. M.: Spatial and temporal trends of  
941 precipitation chemistry in the United States, 1985-2002, *Environ. Pollut.*, 135, 347-361,  
942 doi:10.1016/j.envpol.2004.11.016, 2005.

943

944 Lehmann, C. M. B., and Gay, D. A.: Monitoring long-term trends of acidic wet deposition in US  
945 precipitation: Results from the National Atmospheric Deposition Program, *PowerPlant*  
946 *Chemistry*, 13(7), 2011.

947

948 Levin, Z., Ganor, E., and Gladstein, V.: The effects of desert particles coated with sulfate on rain  
949 formation in the eastern Mediterranean, *J. Appl. Meteorol.*, 35, 1511-1523, 1996.

950

951 Likens, G.: Acid rain. In: *Encyclopedia of Earth*, Eds. Cutler J. Cleveland (Washington, D.C.:  
952 Environmental Information Coalition, National Council for Science and the Environment).  
953 [http://www.eoearth.org/article/Acid\\_rain](http://www.eoearth.org/article/Acid_rain), 2007.

954

955 Liptzin, D., and Seastedt, T. R.: Regional and local patterns of soil nutrients at Rocky Mountain  
956 treelines, *Geoderma*, 160, 208-217, 2010.

957

958 Loye-Pilot, M. D., and Morelli, J.: Fluctuations of ionic composition of precipitations collected  
959 in corsica related to changes in the origins of incoming aerosols, *J. Aerosol Sci.*, 19, 577-585,  
960 1988.

961

962 Lynch, J. A., Grimm, J. W., and Bowersox, V. C.: Trends in precipitation chemistry in the  
963 United-States - a national perspective, 1980-1992, *Atmos. Environ.*, 29, 1231-1246,  
964 doi:10.1016/1352-2310(94)00371-Q, 1995.

965

966 Mahowald, N., Jickells, T. D., Baker, A. R., Artaxo, P., Benitez-Nelson, C. R., Bergametti, G.,  
967 Bond, T. C., Chen, Y., Cohen, D. D., Herut, B., Kubilay, N., Losno, R., Luo, C., Maenhaut, W.,  
968 McGee, K. A., Okin, G. S., Siefert, R. L., and Tsukuda, S.: Global distribution of atmospheric  
969 phosphorus sources, concentrations and deposition rates, and anthropogenic impacts, *Global*  
970 *Biogeochem. Cy.*, 22, Gb4026, doi:10.1029/2008gb003240, 2008.

971

972 Malm, W. C., Sisler, J. F., Huffman, D., Eldred, R. A., and Cahill, T. A.: Spatial and Seasonal  
973 Trends in Particle Concentration and Optical Extinction in the United-States, *J. Geophys. Res.*,  
974 99, 1347-1370, doi:10.1029/93jd02916, 1994.

975

976 Malm, W. C., Day, D. E., Kreidenweis, S. M., Collett, J. L., and Lee, T.: Humidity-dependent  
977 optical properties of fine particles during the Big Bend regional aerosol and visibility  
978 observational study, *J. Geophys. Res.*, 108, 4279, doi:10.1029/2002jd002998, 2003.

979

980 Malm, W. C., Schichtel, B. A., Pitchford, M. L., Ashbaugh, L. L., and Eldred, R. A.: Spatial and  
981 monthly trends in speciated fine particle concentration in the United States, *J. Geophys. Res.*,  
982 109, D03306, doi:10.1029/2003jd003739, 2004.

983

984 Matichuk, R., Barbaris, B., Betterton, E. A., Hori, M., Murao, N., Ohta, S., and Ward, D.: A  
985 decade of aerosol and gas precursor chemical characterization at Mt. Lemmon, Arizona (1992 to  
986 2002), *J. Meteorol. Soc. Jpn.*, 84, 653-670, 2006.

987

988 Matsuki, A., Schwarzenboeck, A., Venzac, H., Laj, P., Crumeyrolle, S., and Gomes, L.: Cloud  
989 processing of mineral dust: direct comparison of cloud residual and clear sky particles during  
990 AMMA aircraft campaign in summer 2006, *Atmos. Chem. Phys.*, 10, 1057-1069,  
991 doi:10.5194/acp-10-1057-2010, 2010.

992

993 Migliavacca, D., Teixeira, E. C., Pires, M., and Fachel, J.: Study of chemical elements in  
994 atmospheric precipitation in South Brazil, *Atmos. Environ.*, 38, 1641-1656, 2004.

995

996 Migliavacca, D., Teixeira, E. C., Wiegand, F., Machado, A. C. M., and Sanchez, J.: Atmospheric  
997 precipitation and chemical composition of an urban site, Guaiba hydrographic basin, Brazil,  
998 *Atmos. Environ.*, 39, 1829-1844, 2005.

999

1000 Morales-Baquero, R., Pulido-Villena, E., and Reche, I.: Atmospheric inputs of phosphorus and  
1001 nitrogen to the southwest Mediterranean region: Biogeochemical responses of high mountain  
1002 lakes, *Limnol. Oceanogr.*, 51, 830-837, 2006.

1003

1004 Mouli, P. C., Mohan, S. V., and Reddy, S. J.: Rainwater chemistry at a regional representative  
1005 urban site: influence of terrestrial sources on ionic composition, *Atmos. Environ.*, 39, 999-1008,  
1006 2005.

1007

1008 Neff, J. C., Reynolds, R. L., Belnap, J., and Lamothe, P.: Multi-decadal impacts of grazing on  
1009 soil physical and biogeochemical properties in southeast Utah, *Ecol. Appl.*, 15, 87-95, 2005.

1010

1011 Neff, J. C., Ballantyne, A. P., Farmer, G. L., Mahowald, N. M., Conroy, J. L., Landry, C. C.,  
1012 Overpeck, J. T., Painter, T. H., Lawrence, C. R., and Reynolds, R. L.: Increasing eolian dust  
1013 deposition in the western United States linked to human activity, *Nat. Geosci.*, 1, 189-195, 2008.

1014

1015 Nilles, M. A., and Conley, B. E.: Changes in the chemistry of precipitation in the United States,  
1016 1981-1998, *Water Air Soil Poll.*, 130, 409-414, doi:10.1023/A:1013889302895, 2001.

1017

1018 Okin, G. S., Mahowald, N., Chadwick, O. A., and Artaxo, P.: Impact of desert dust on the  
1019 biogeochemistry of phosphorus in terrestrial ecosystems, *Global Biogeochem. Cy.*, 18, Gb2005,  
1020 doi:10.1029/2003gb002145, 2004.

1021

1022 Olivier, S., Blaser, C., Brutsch, S., Frolova, N., Gaggeler, H. W., Henderson, K. A., Palmer, A.  
1023 S., Papina, T., and Schwikowski, M.: Temporal variations of mineral dust, biogenic tracers, and  
1024 anthropogenic species during the past two centuries from Belukha ice core, Siberian Altai, *J.*  
1025 *Geophys. Res.*, 111, D05309, doi:10.1029/2005jd005830, 2006.

1026

1027 Painter, T. H., Barrett, A. P., Landry, C. C., Neff, J. C., Cassidy, M. P., Lawrence, C. R.,  
1028 McBride, K. E., and Farmer, G. L.: Impact of disturbed desert soils on duration of mountain  
1029 snow cover, *Geophys. Res. Lett.*, 34, L12502, doi:10.1029/2007gl030284, 2007.

1030

1031 Painter, T. H., Deems, J. S., Belnap, J., Hamlet, A. F., Landry, C. C., and Udall, B.: Response of  
1032 Colorado River runoff to dust radiative forcing in snow, *P. Natl. Acad. Sci. USA*, 107, 17125-  
1033 17130, doi:10.1073/pnas.0913139107, 2010.

1034

1035 Prenni, A. J., Petters, M. D., Kreidenweis, S. M., Heald, C. L., Martin, S. T., Artaxo, P., Garland,  
1036 R. M., Wollny, A. G., and Poschl, U.: Relative roles of biogenic emissions and Saharan dust as  
1037 ice nuclei in the Amazon basin, *Nat. Geosci.*, 2, 401-404, 2009.

1038

1039 Preunkert, S., Wagenbach, D., and Legrand, M.: A seasonally resolved alpine ice core record of  
1040 nitrate: Comparison with anthropogenic inventories and estimation of preindustrial emissions of  
1041 NO in Europe, *J. Geophys. Res.*, 108, 4681, doi:10.1029/2003jd003475, 2003.

1042

1043 Psenner, R.: Living in a dusty world: Airborne dust as a key factor for alpine lakes, *Water Air*  
1044 *Soil Poll.*, 112, 217-227, 1999.

1045

1046 Qin, G. Y., and Huang, M. Y.: A study on rain acidification processes in ten cities of China,  
1047 *Water Air Soil Poll.*, 130, 163-174, 2001.

1048

1049 Raman, R. S., and Ramachandran, S.: Source apportionment of the ionic components in  
1050 precipitation over an urban region in Western India, *Environ. Sci. Pollut. R.*, 18, 212-225, 2011.  
1051

1052 Reynolds, R., Belnap, J., Reheis, M., Lamothe, P., and Luiszer, F.: Aeolian dust in Colorado  
1053 Plateau soils: Nutrient inputs and recent change in source, *P. Natl. Acad. Sci. USA*, 98, 7123-  
1054 7127, 2001.  
1055

1056 Rhoades, C., Elder, K., and Greene, E.: The influence of an extensive dust event on snow  
1057 chemistry in the Southern Rocky Mountains, *Arct. Antarct. Alp. Res.*, 42, 98-105, 2010.  
1058

1059 Rosenfeld, D., Rudich, Y., and Lahav, R.: Desert dust suppressing precipitation: A possible  
1060 desertification feedback loop, *P. Natl. Acad. Sci. USA*, 98, 5975-5980, 2001.  
1061

1062 Rosenfeld, D., and Givati, A.: Evidence of orographic precipitation suppression by air pollution-  
1063 induced aerosols in the western United States, *J. Appl. Meteorol. Clim.*, 45, 893-911, 2006.  
1064

1065 Safai, P. D., Rao, P. S. P., Mornin, G. A., All, K., Chate, D. M., and Praveen, P. S.: Chemical  
1066 composition of precipitation during 1984-2002 at Pune, India, *Atmos. Environ.*, 38, 1705-1714,  
1067 2004.  
1068

1069 Sassen, K., DeMott, P. J., Prospero, J. M., and Poellot, M. R.: Saharan dust storms and indirect  
1070 aerosol effects on clouds: CRYSTAL-FACE results, *Geophys. Res. Lett.*, 30, 1633,  
1071 doi:10.1029/2003gl017371, 2003.  
1072

1073 Satyanarayana, J., Reddy, L. A. K., Kulshrestha, M. J., Rao, R. N., and Kulshrestha, U. C.:  
1074 Chemical composition of rain water and influence of airmass trajectories at a rural site in an  
1075 ecological sensitive area of Western Ghats (India), *J. Atmos. Chem.*, 66, 101-116,  
1076 doi:10.1007/s10874-011-9193-2, 2010.  
1077

1078 Schichtel, B. A., Malm, W. C., Bench, G., Fallon, S., McDade, C. E., Chow, J. C., and Watson,  
1079 J. G.: Fossil and contemporary fine particulate carbon fractions at 12 rural and urban sites in the  
1080 United States, *J. Geophys. Res.*, 113, D02311, doi:10.1029/2007jd008605, 2008.  
1081

1082 Schlesinger, W. H., Reynolds, J. F., Cunningham, G. L., Huenneke, L. F., Jarrell, W. M.,  
1083 Virginia, R. A., and Whitford, W. G.: Biological feedbacks in global desertification, *Science*,  
1084 247, 1043-1048, 1990.  
1085

1086 Schwikowski, M., Seibert, P., Baltensperger, U., and Gaggeler, H. W.: A study of an outstanding  
1087 saharan dust event at the high-alpine site Jungfraujoch, Switzerland, *Atmos. Environ.*, 29, 1829-  
1088 1842, 1995.  
1089

1090 Schwikowski, M., Doscher, A., Gaggeler, H. W., and Schotterer, U.: Anthropogenic versus  
1091 natural sources of atmospheric sulphate from an Alpine ice core, *Tellus B*, 51, 938-951, 1999.  
1092

1093 Seager, R., and Vecchi, G. A.: Greenhouse warming and the 21st century hydroclimate of  
1094 southwestern North America, *P. Natl. Acad. Sci. USA*, 107, 21277-21282,  
1095 doi:10.1073/pnas.0910856107, 2010.  
1096  
1097 Seinfeld, J. H. and Pandis, S. N.: *Atmospheric Chemistry and Physics*, Second Edition, Wiley-  
1098 Interscience, New York, 2006.  
1099  
1100 Singh, K. P., Singh, V. K., Malik, A., Sharma, N., Murthy, R. C., and Kumar, R.:  
1101 Hydrochemistry of wet atmospheric precipitation over an urban area in northern Indo-gangetic  
1102 plains, *Environ. Monit. Assess.*, 131, 237-254, 2007.  
1103  
1104 Sirois, A., Vet, R., and Lamb, D.: A comparison of the precipitation chemistry measurements  
1105 obtained by the CAPMoN and NADP/NTN networks, *Environ. Monit. Assess.*, 62, 273-303, doi  
1106 10.1023/A:1006272609744, 2000.  
1107  
1108 Skiles, S. M., Painter, T. H., Deems, J. S., Bryant, A. C., and Landry, C. C.: Dust radiative  
1109 forcing in snow of the Upper Colorado River Basin: 2. Interannual variability in radiative forcing  
1110 and snowmelt rates, *Water Resour. Res.*, 48, W07522, doi:10.1029/2012wr011986, 2012.  
1111  
1112 Sorooshian, A., Murphy, S. N., Hersey, S., Gates, H., Padro, L. T., Nenes, A., Brechtel, F. J.,  
1113 Jonsson, H., Flagan, R. C., and Seinfeld, J. H.: Comprehensive airborne characterization of  
1114 aerosol from a major bovine source, *Atmos. Chem. Phys.*, 8, 5489-5520, 2008.  
1115  
1116 Sorooshian, A., Wonaschütz, A., Jarjour, E. G., Hashimoto, B. I., Schichtel, B. A., and Betterton,  
1117 E. A.: An aerosol climatology for a rapidly growing arid region (southern Arizona): Major  
1118 aerosol species and remotely sensed aerosol properties, *J. Geophys. Res.*, 116, 19205,  
1119 doi:10.1029/2011jd016197, 2011.  
1120  
1121 Sorooshian, A., Csavina, J., Shingler, T., Dey, S., Brechtel, F. J., Saez, A. E., and Betterton, E.  
1122 A.: Hygroscopic and chemical properties of aerosols collected near a copper smelter:  
1123 implications for public and environmental health, *Environ. Sci. Technol.*, 46, 9473-9480, 2012.  
1124  
1125 Stoorvogel, J. J., VanBreemen, N., and Janssen, B. H.: The nutrient input by Harmattan dust to a  
1126 forest ecosystem in Cote d'Ivoire, Africa, *Biogeochemistry*, 37, 145-157, 1997.  
1127  
1128 Sullivan, R. C., Guazzotti, S. A., Sodeman, D. A., and Prather, K. A.: Direct observations of the  
1129 atmospheric processing of Asian mineral dust, *Atmos. Chem. Phys.*, 7, 1213-1236,  
1130 doi:10.5194/acp-7-1213-2007, 2007.  
1131  
1132 Teixeira, E. C., Migliavacca, D., Pereira, S., Machado, A. C. M., and Dallarosa, J. B.: Study of  
1133 wet precipitation and its chemical composition in South of Brazil, *An. Acad. Bras. Cienc.*, 80,  
1134 381-395, 2008.  
1135  
1136 Tong, D. Q., Dan, M., Wang, T., and Lee, P.: Long-term dust climatology in the western United  
1137 States reconstructed from routine aerosol ground monitoring, *Atmos. Chem. Phys.*, 12, 5189-  
1138 5205, 2012.

1139  
1140 Topcu, S., Incecik, S., and Atimtay, A. T.: Chemical composition of rainwater at EMEP station  
1141 in Ankara, Turkey, *Atmos. Res.*, 65, 77-92, 2002.  
1142  
1143 Torres, O., Bhartia, P. K., Herman, J. R., Ahmad, Z., and Gleason, J.: Derivation of aerosol  
1144 properties from satellite measurements of backscattered ultraviolet radiation: Theoretical basis, *J.*  
1145 *Geophys. Res.*, 103, 17099-17110, 1998.  
1146  
1147 Turk, J. T., Taylor, H. E., Ingersoll, G. P., Tonnessen, K. A., Clow, D. W., Mast, M. A.,  
1148 Campbell, D. H., and Melack, J. M.: Major-ion chemistry of the Rocky Mountain snowpack,  
1149 USA, *Atmos. Environ.*, 35, 3957-3966, 2001.  
1150  
1151 Twohy, C. H., and Gandrud, B. W.: Electron microscope analysis of residual particles from  
1152 aircraft contrails, *Geophys. Res. Lett.*, 25, 1359-1362, 1998.  
1153  
1154 VanCuren, R. A., and Cahill, T. A.: Asian aerosols in North America: Frequency and  
1155 concentration of fine dust, *J. Geophys. Res.*, 107, 4804, doi:10.1029/2002jd002204, 2002.  
1156  
1157 van der Swaluw, E., Asman, W. A. H., van Jaarsveld, H., and Hoogerbrugge, R.: Wet deposition  
1158 of ammonium, nitrate and sulfate in the Netherlands over the period 1992-2008, *Atmos.*  
1159 *Environ.*, 45, 3819-3826, 2011.  
1160  
1161 Vicars, W. C., and Sickman, J. O.: Mineral dust transport to the Sierra Nevada, California:  
1162 Loading rates and potential source areas, *J. Geophys. Res.*, 116, G01018,  
1163 doi:10.1029/2010jg001394, 2011.  
1164  
1165 Wake, C. P., Mayewski, P. A., and Spencer, M. J.: A review of central Asian glaciochemical  
1166 data, *Ann. Glaciol.*, 14, 301-306, 1990.  
1167  
1168 Wake, C. P., Mayewski, P. A., Wang, P., Yang, Q. H., Han, J. K., and Xie, Z. H.: Anthropogenic  
1169 sulfate and Asian dust signals in snow from Tien-Shan, northwest China, *Ann. Glaciol.*, 16, 45-  
1170 52, 1992.  
1171  
1172 Wells, K. C., Witek, M., Flatau, P., Kreidenweis, S. M., and Westphal, D. L.: An analysis of  
1173 seasonal surface dust aerosol concentrations in the western US (2001-2004): Observations and  
1174 model predictions, *Atmos. Environ.*, 41, 6585-6597, 2007.  
1175  
1176 Williams, M. W., and Melack, J. M.: Solute chemistry of snowmelt and runoff in an alpine basin,  
1177 Sierra-Nevada, *Water Resour. Res.*, 27, 1575-1588, 1991.  
1178  
1179 Wolfe, A. P., Van Gorp, A. C., and Baron, J. S.: Recent ecological and biogeochemical changes  
1180 in alpine lakes of Rocky Mountain National Park (Colorado, USA): a response to anthropogenic  
1181 nitrogen deposition, *Geobiology*, 1, 153-168, 2003.  
1182  
1183 Wonaschütz, A., Hersey, S. P., Sorooshian, A., Craven, J. S., Metcalf, A. R., Flagan, R. C., and  
1184 Seinfeld, J. H.: Impact of a large wildfire on water-soluble organic aerosol in a major urban area:

1185 the 2009 Station Fire in Los Angeles County, *Atmos. Chem. Phys.*, 11, 8257-8270,  
1186 doi:10.5194/acp-11-8257-2011, 2011.  
1187  
1188 Woodhouse, C. A., Meko, D. M., MacDonald, G. M., Stahle, D. W., and Cooke, E. R.: A 1,200-  
1189 year perspective of 21st century drought in southwestern North America, *P. Natl. Acad. Sci.*  
1190 *USA*, 107, 21283-21288, doi:10.1073/pnas.0911197107, 2010.  
1191  
1192 Yeung, M. C., Lee, S. C., Lun, B. H., and Tanner, P. A.: Summer rain events in south-east Asia:  
1193 Spatial and temporal variations, *Atmos. Res.*, 86, 241-248, 2007.  
1194  
1195 Yi, L., Xiaolan, Y., Hongbing, C., Weili, L., Jie, T., and Shufeng, W.: Chemical characteristics  
1196 of precipitation at three Chinese regional background stations from 2006 to 2007, *Atmos. Res.*,  
1197 96, 173-183, 2010.  
1198  
1199 Youn, J. -S., Wang, Z., Wonaschütz, A., Arellano, A., Betterton, E. A., and Sorooshian, A.:  
1200 Evidence of aqueous secondary organic aerosol formation from biogenic emissions in the North  
1201 American Sonoran Desert, *Geophys. Res. Lett.*, in press, 2013.  
1202  
1203 Yu, X. Y., Taehyoung, L., Ayres, B., Kreidenweis, S. M., Collett, J. L., and Malm, W.:  
1204 Particulate nitrate measurement using nylon filters, *J. Air Waste Manage.*, 55, (8), 1100-1110,  
1205 2005.  
1206  
1207 Zhang, M. Y., Wang, S. J., Wu, F. C., Yuan, X. H., and Zhang, Y.: Chemical compositions of  
1208 wet precipitation and anthropogenic influences at a developing urban site in southeastern China,  
1209 *Atmos. Res.*, 84, 311-322, 2007.  
1210  
1211 Zhang, Y. L., Kang, S. C., Li, C. L., Cong, Z. Y., and Zhang, Q. G.: Wet deposition of  
1212 precipitation chemistry during 2005-2009 at a remote site (Nam Co Station) in central Tibetan  
1213 Plateau, *J. Atmos. Chem.*, 69, 187-200, 2012.  
1214  
1215 Zhao, H. B., Xu, B. Q., Yao, T. D., Tian, L. D., and Li, Z.: Records of sulfate and nitrate in an  
1216 ice core from Mount Muztagata, central Asia, *J. Geophys. Res.*, 116, D13304,  
1217 doi:10.1029/2011jd015735, 2011.  
1218  
1219 Zimmermann, F., Weinbruch, S., Schutz, L., Hofmann, H., Ebert, M., Kandler, K., and  
1220 Worringer, A.: Ice nucleation properties of the most abundant mineral dust phases, *J. Geophys.*  
1221 *Res.*, 113, D23204, doi:10.1029/2008jd010655, 2008.  
1222  
1223  
1224  
1225  
1226  
1227  
1228  
1229  
1230

1231 **Table 1.** Summary of co-located aerosol (IMPROVE) and precipitation (NADP/NTN) data used  
 1232 with coordinates, altitudes, and range of full years in which data are analyzed. The location of  
 1233 sites is shown in Fig. 1. “NP” and “NM” refer to National Park and National Monument,  
 1234 respectively. Altitudes are ASL.  
 1235

Station	State	Lat (°)	Lon (°)	Alt (m)	Data Analysis Range
Mesa Verde NP (NTN)	CO	37.198	-108.5	2162	1995-2010
Mesa Verde NP (IMPROVE)	CO	37.198	-108.5	2172	
Chiricahua (NTN)	AZ	32.010	-109.4	1570	2000-2010
Chiricahua NM (IMPROVE)	AZ	32.009	-109.4	1555	
Organ Pipe Cactus NM (NTN)	AZ	31.949	-112.8	501	2003-2010
Organ Pipe (IMPROVE)	AZ	31.951	-112.8	504	
Bryce Canyon NP (NTN)	UT	37.619	-112.2	2477	1995-2010
Bryce Canyon NP (IMPROVE)	UT	37.618	-112.2	2481	
Gila Cliff Dwellings NM (NTN)	NM	33.220	-108.2	1772	1995-2010
Gila Wilderness (IMPROVE)	NM	33.220	-108.2	1776	
Bandelier NM (NTN)	NM	35.779	-106.3	1997	1995-2010
Bandelier NM (IMPROVE)	NM	35.780	-106.3	1988	

1236  
 1237  
 1238  
 1239  
 1240  
 1241  
 1242  
 1243  
 1244  
 1245  
 1246  
 1247  
 1248  
 1249  
 1250  
 1251  
 1252  
 1253  
 1254  
 1255  
 1256  
 1257  
 1258  
 1259  
 1260  
 1261  
 1262  
 1263

1264 **Table 2.** Correlation matrix (r values) for rain water constituent concentrations measured at  
 1265 Organ Pipe between 2003 and 2010 and snow water constituent concentrations measured at  
 1266 Bandelier between 1995 and 2010. Values are only shown when statistically significant (95%)  
 1267 with a two-tailed Student's T-Test. Refer to Supplementary Information for all data for the six  
 1268 sites.  
 1269

	Organ Pipe Rain (n = 107)									Bandelier Snow (n = 90)								
	Ca	Mg	K	Na	NH <sub>4</sub>	NO <sub>3</sub>	Cl	SO <sub>4</sub>	pH	Ca	Mg	K	Na	NH <sub>4</sub>	NO <sub>3</sub>	Cl	SO <sub>4</sub>	pH
Ca	1.00									1.00								
Mg	0.76	1.00								0.87	1.00							
K	0.92	0.82	1.00							0.83	0.84	1.00						
Na	0.59	0.96	0.68	1.00						0.68	0.76	0.70	1.00					
NH <sub>4</sub>	0.21	--	0.25	--	1.00					--	0.23	0.29	0.45	1.00				
NO <sub>3</sub>	0.28	--	0.34	--	0.89	1.00				0.28	0.36	0.41	0.43	0.61	1.00			
Cl	0.59	0.96	0.68	1.00	--	--	1.00			0.48	0.61	0.53	0.85	0.44	0.38	1.00		
SO <sub>4</sub>	0.47	0.45	0.56	0.28	0.67	0.79	0.26	1.00		0.36	0.48	0.49	0.60	0.81	0.51	0.60	1.00	
pH	0.44	0.54	0.49	0.50	--	--	0.51	--	1.00	0.72	0.72	0.65	0.43	--	--	0.21	--	1.00

1270  
 1271  
 1272  
 1273  
 1274  
 1275  
 1276  
 1277  
 1278  
 1279  
 1280  
 1281  
 1282  
 1283  
 1284  
 1285  
 1286  
 1287  
 1288  
 1289  
 1290  
 1291  
 1292  
 1293  
 1294  
 1295  
 1296  
 1297  
 1298  
 1299

1300 **Table 3.** Correlation (r) of aerosol mass concentrations (fine soil, sulfate) and the coarse:fine  
 1301 mass concentration ratio with precipitation species mass concentrations. Values are only shown  
 1302 when statistically significant (95%) with a two-tailed Student's T-Test. There are no snow data at  
 1303 Organ Pipe. The sample range for data below is 39 - 240.  
 1304

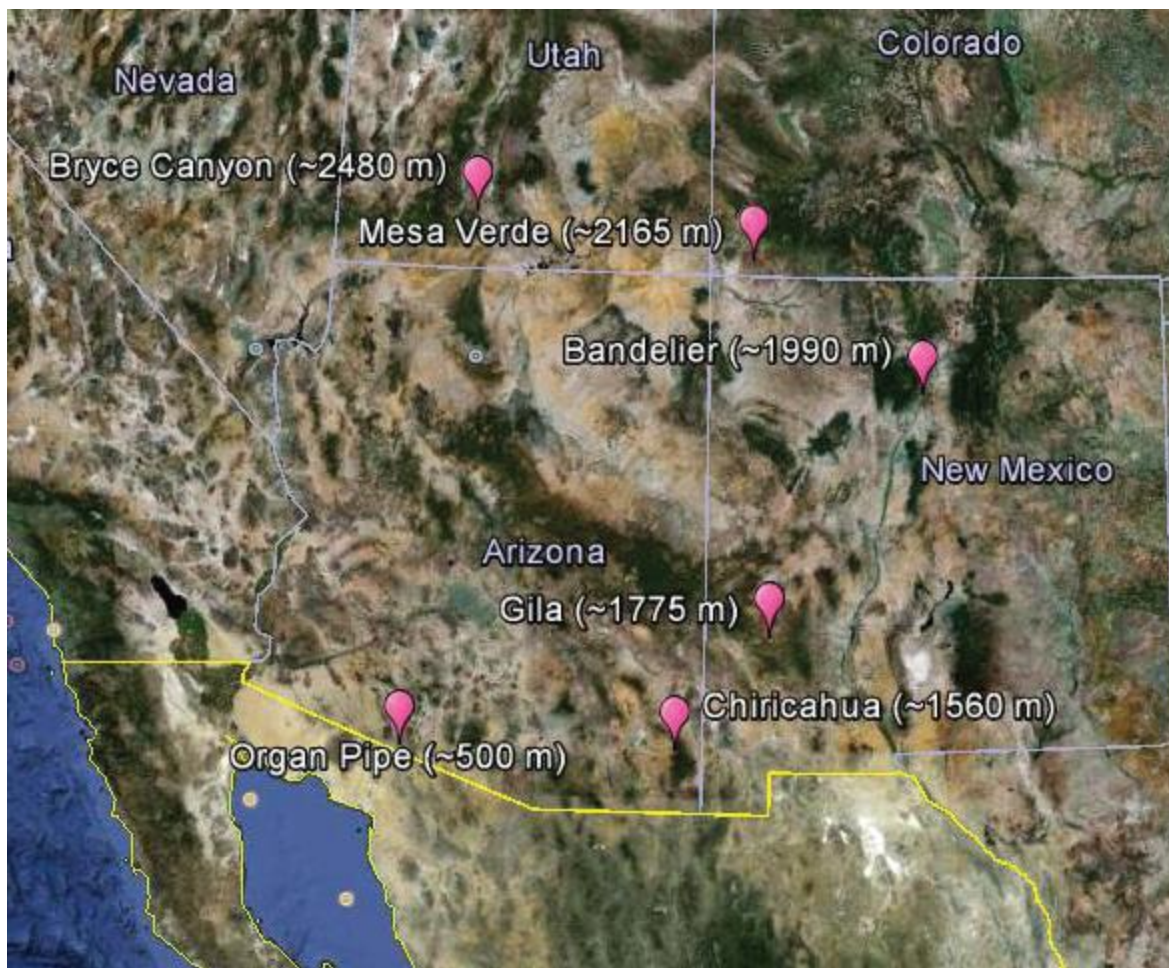
	Particulate Fine Soil						Particulate Sulfate						Coarse:Fine Mass Ratio					
	Band	BC	Chi	Gila	MV	OP	Band	BC	Chi	Gila	MV	OP	Band	BC	Chi	Gila	MV	OP
Rain Ca	0.27	0.40	0.33	0.32	0.15	--	--	0.23	--	--	--	--	--	--	--	--	0.18	--
Rain Mg	0.39	0.45	0.25	0.34	0.20	--	--	0.22	--	--	--	--	--	--	--	0.12	--	--
Rain K	--	0.23	0.23	0.15	0.31	--	--	--	--	--	--	--	--	--	--	--	0.16	--
Rain Na	0.33	0.36	--	0.18	0.20	--	--	0.29	--	--	--	--	--	--	--	--	--	--
Rain NH <sub>4</sub>	--	0.22	0.26	0.16	--	0.23	--	0.18	0.19	0.21	--	0.30	-0.16	--	--	-0.13	--	--
Rain NO <sub>3</sub>	--	0.30	0.31	0.21	--	0.25	--	0.30	0.23	0.26	--	0.32	-0.17	--	--	--	--	--
Rain Cl	0.32	0.37	--	0.20	0.22	--	--	0.34	--	--	--	--	--	--	--	0.14	--	--
Rain SO <sub>4</sub>	--	0.28	0.23	0.19	--	0.24	0.14	0.41	--	0.39	0.20	0.29	--	--	--	--	--	--
Snow Ca	--	0.23	--	0.73	0.74	--	--	--	--	--	-0.21	--	0.22	0.19	--	0.63	0.27	--
Snow Mg	--	0.26	--	0.73	0.56	--	--	--	--	--	-0.24	--	0.30	0.19	--	0.65	0.28	--
Snow K	--	--	--	0.70	0.39	--	--	--	--	--	-0.19	--	0.30	--	--	0.72	0.28	--
Snow Na	--	--	--	0.59	--	--	--	--	--	--	--	--	0.34	0.17	--	0.57	0.27	--
Snow NH <sub>4</sub>	--	0.18	--	0.38	--	--	--	--	--	--	--	--	--	--	--	0.36	--	--
Snow NO <sub>3</sub>	--	--	--	0.46	--	--	--	0.15	--	--	--	--	0.22	--	--	0.48	--	--
Snow Cl	--	--	--	0.59	--	--	--	--	--	--	--	--	--	--	--	0.60	0.23	--
Snow SO <sub>4</sub>	--	0.24	--	0.61	0.34	--	--	0.18	--	--	--	--	--	--	--	0.57	--	--

1305  
 1306  
 1307  
 1308  
 1309  
 1310  
 1311  
 1312  
 1313  
 1314  
 1315  
 1316  
 1317  
 1318  
 1319  
 1320  
 1321  
 1322  
 1323  
 1324  
 1325  
 1326  
 1327  
 1328  
 1329  
 1330

1331 **Table 4.** Long-term trend analysis for the Southwest monsoon season (JAS). Slopes of each  
 1332 parameter versus year are shown with correlation coefficients ( $r^2$ ) of the linear best fit line in  
 1333 parenthesis. Units are  $\mu\text{g m}^{-3} \text{y}^{-1}$  for the aerosol species,  $\text{mg L}^{-1} \text{y}^{-1}$  for the rain species, and  $\text{y}^{-1}$   
 1334 for the coarse:fine ratio,  $\text{NO}_3^-:\text{SO}_4^{2-}$  ratio, and pH. No other common aerosol and rain water  
 1335 species are shown as they do not have statistically significant changes over the durations shown  
 1336 in Table 1.  
 1337

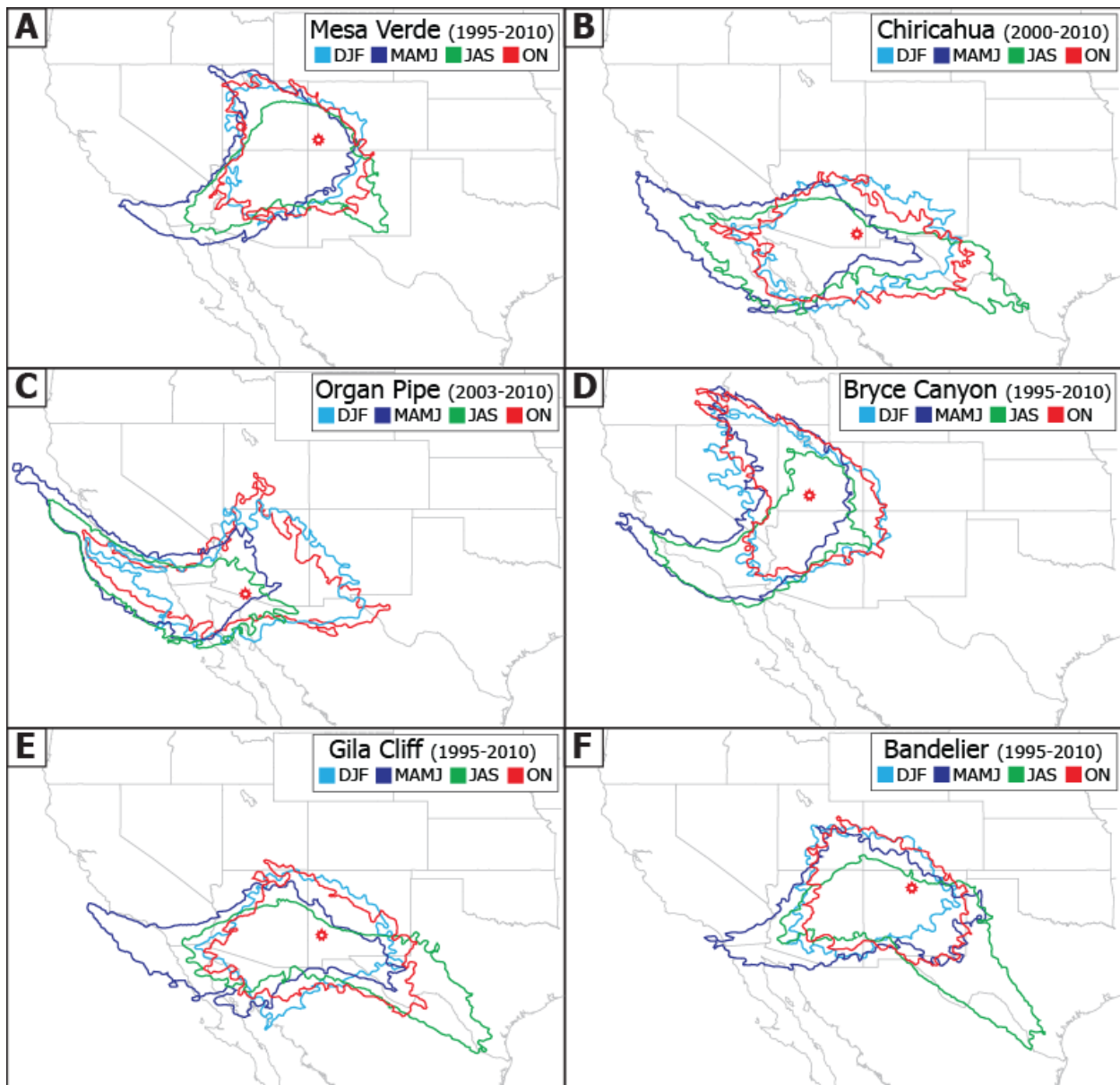
	Bandelier	Bryce Canyon	Chiricahua	Gila Cliff	Mesa Verde	Organ Pipe
Particulate $\text{SO}_4$	-0.037 (0.56)	-0.029 (0.71)	-0.038 (0.52)	-0.047 (0.72)	-0.042 (0.78)	-0.109 (0.80)
Particulate $\text{NO}_3$			-0.006 (0.43)			-0.016 (0.44)
Particulate $\text{NO}_3:\text{SO}_4$					0.005 (0.26)	
Particulate Coarse:Fine						0.084 (0.30)
Rain $\text{SO}_4$		-0.062 (0.28)		-0.057 (0.53)		
Rain $\text{NO}_3$						
Rain $\text{NO}_3:\text{SO}_4$	0.037 (0.33)	0.049 (0.26)		0.065 (0.52)	0.080 (0.81)	
Rain pH	0.028 (0.42)	0.051 (0.32)	0.026 (0.38)	0.034 (0.43)		

1338  
 1339  
 1340  
 1341  
 1342  
 1343  
 1344  
 1345  
 1346  
 1347  
 1348  
 1349  
 1350  
 1351  
 1352  
 1353  
 1354  
 1355  
 1356  
 1357  
 1358  
 1359  
 1360  
 1361  
 1362  
 1363  
 1364  
 1365  
 1366  
 1367  
 1368



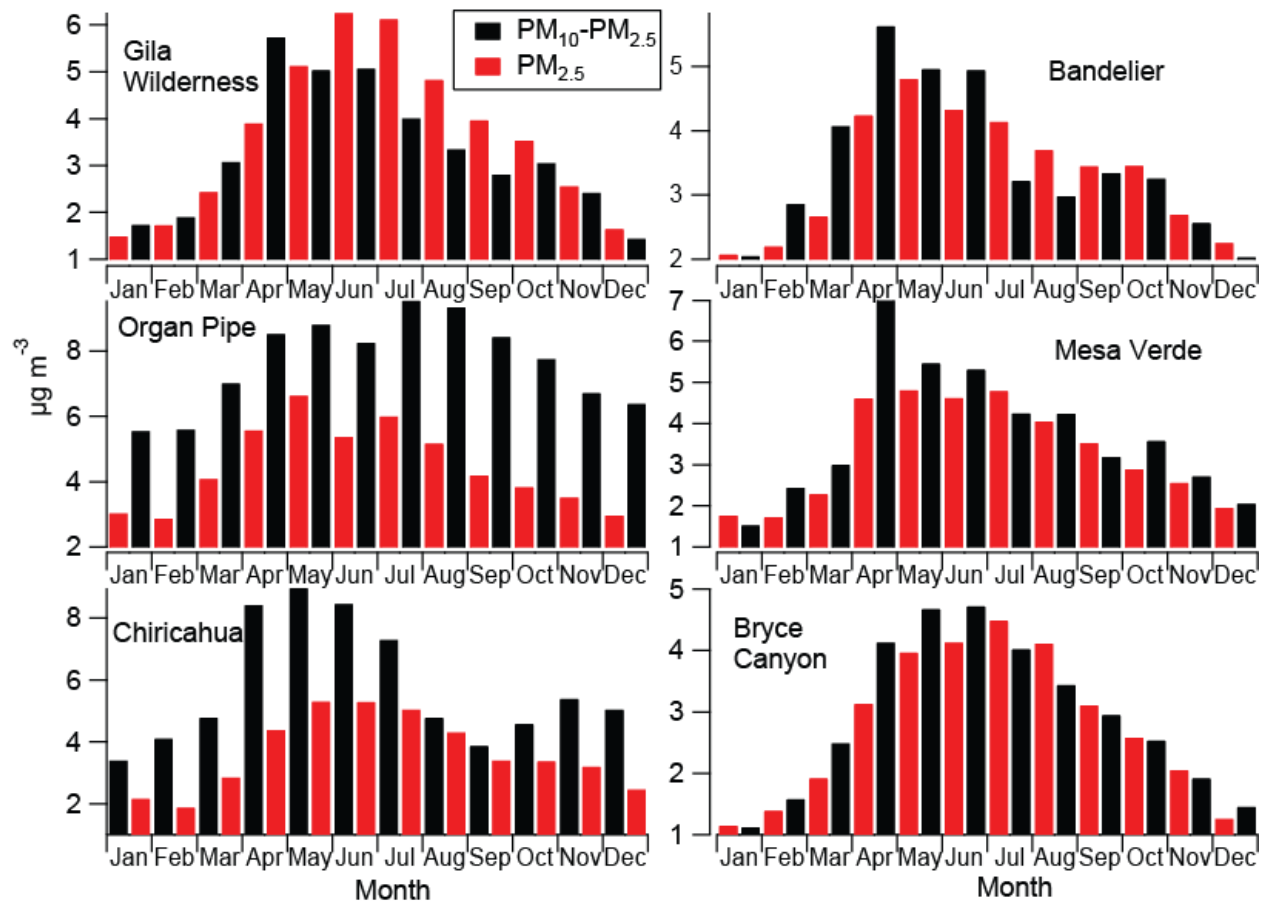
1369  
1370  
1371  
1372  
1373  
1374  
1375  
1376  
1377  
1378  
1379  
1380  
1381  
1382  
1383  
1384  
1385  
1386  
1387  
1388  
1389

**Fig. 1.** Spatial map of co-located EPA IMPROVE and NADP/NTN stations used in this study.



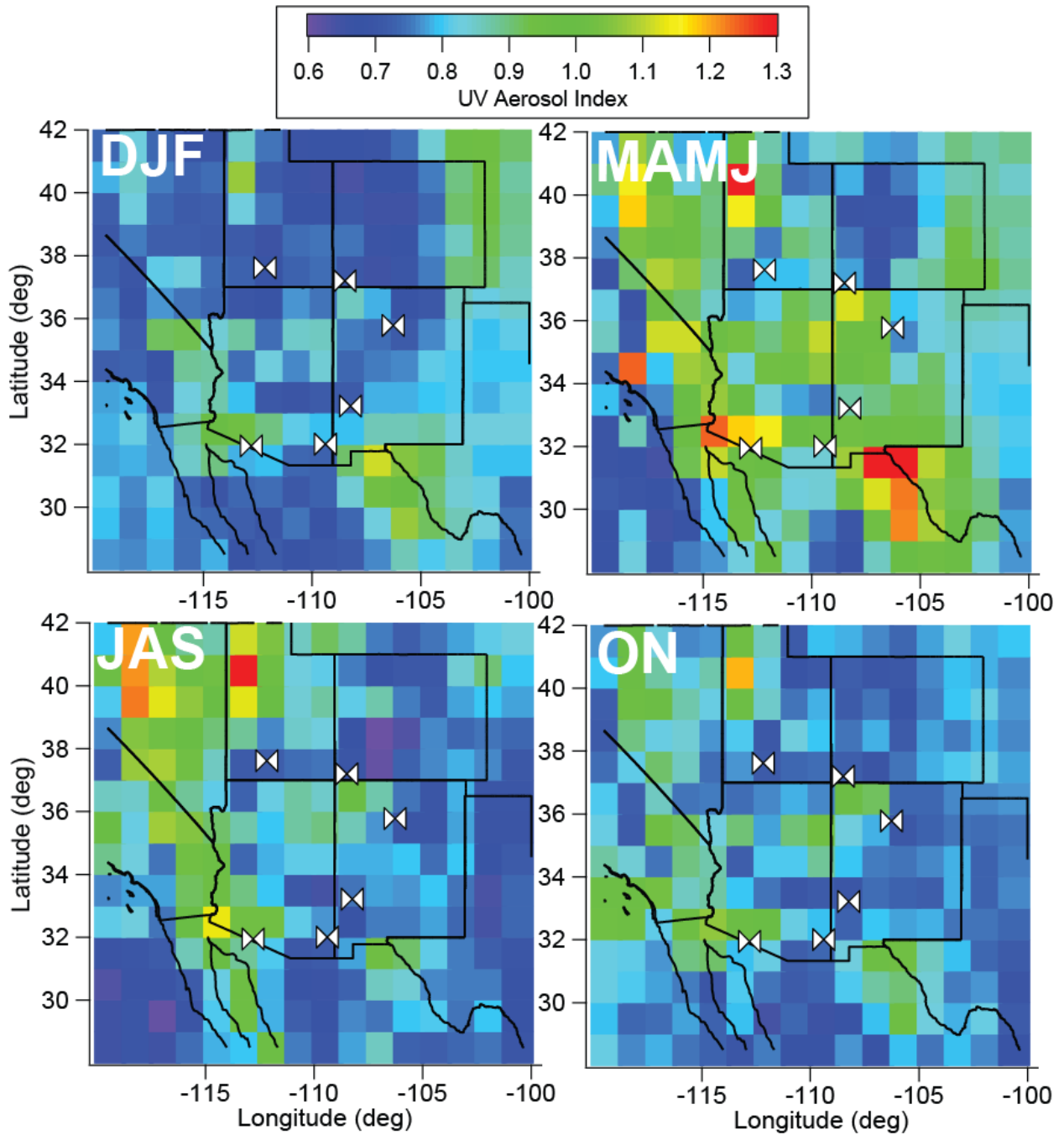
1390  
 1391  
 1392  
 1393  
 1394  
 1395  
 1396  
 1397

**Fig. 2.** Seasonal HYSPLIT data showing the approximate source regions for air parcels ending 10 m AGL at each of the six study sites that are represented by red open markers. The colored borders represent a minimum trajectory frequency of 1% using three-day back-trajectory data, where frequency is defined as the sum of the number of trajectories that passed through each point on the map divided by the number of trajectories analyzed.



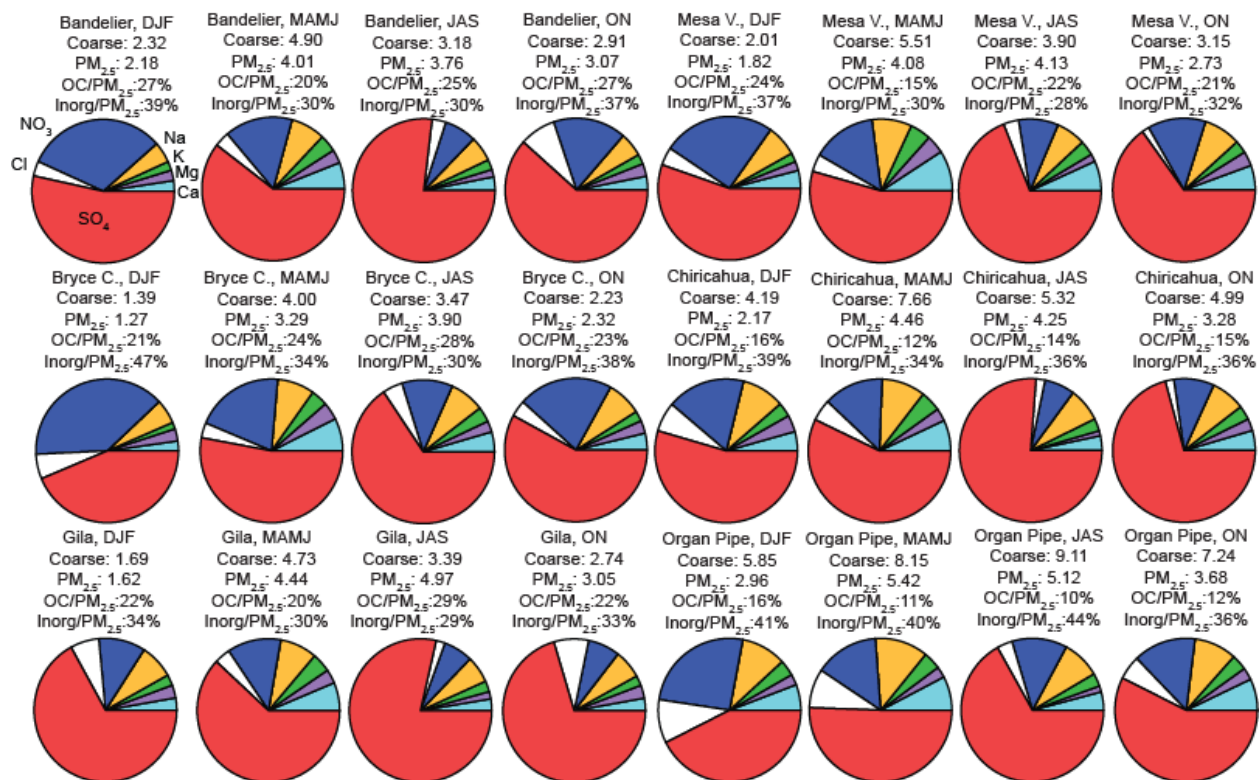
1398  
 1399  
 1400  
 1401  
 1402  
 1403  
 1404  
 1405  
 1406  
 1407  
 1408  
 1409  
 1410  
 1411  
 1412  
 1413  
 1414  
 1415  
 1416  
 1417  
 1418  
 1419

**Fig. 3.** Average monthly fine (PM<sub>2.5</sub>) and coarse (PM<sub>10</sub> - PM<sub>2.5</sub>) aerosol mass concentrations at six EPA IMPROVE sites. These results are based on data ranges shown in Table 1 for each site.



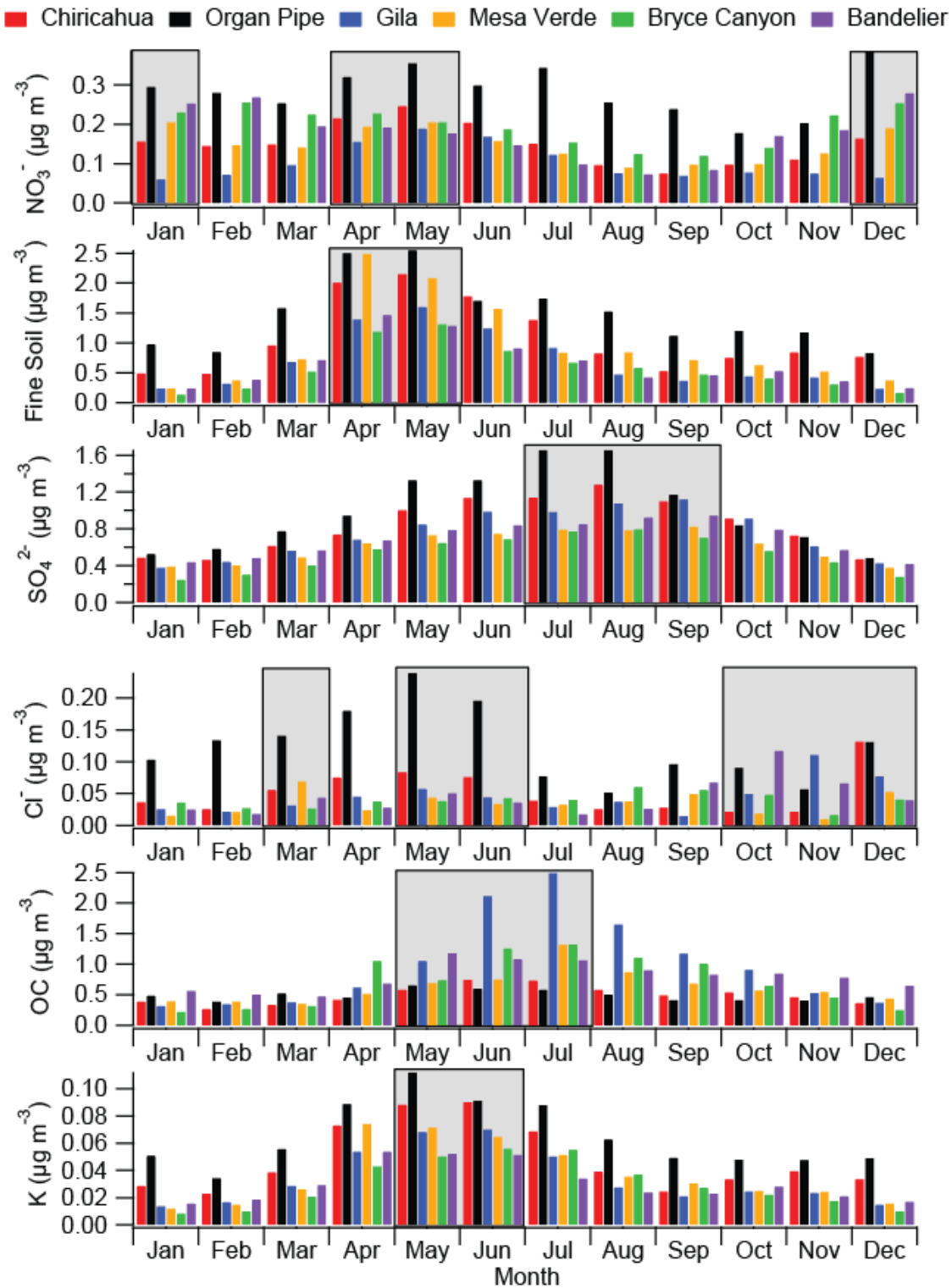
1420  
 1421  
 1422  
 1423  
 1424  
 1425

**Fig. 4.** Average remotely sensed ultraviolet aerosol index values (OMI) in the Southwest between 2005 – 2008 for four seasons. The white markers correspond to the six co-located pairs of IMPROVE and NADP/NTN stations.



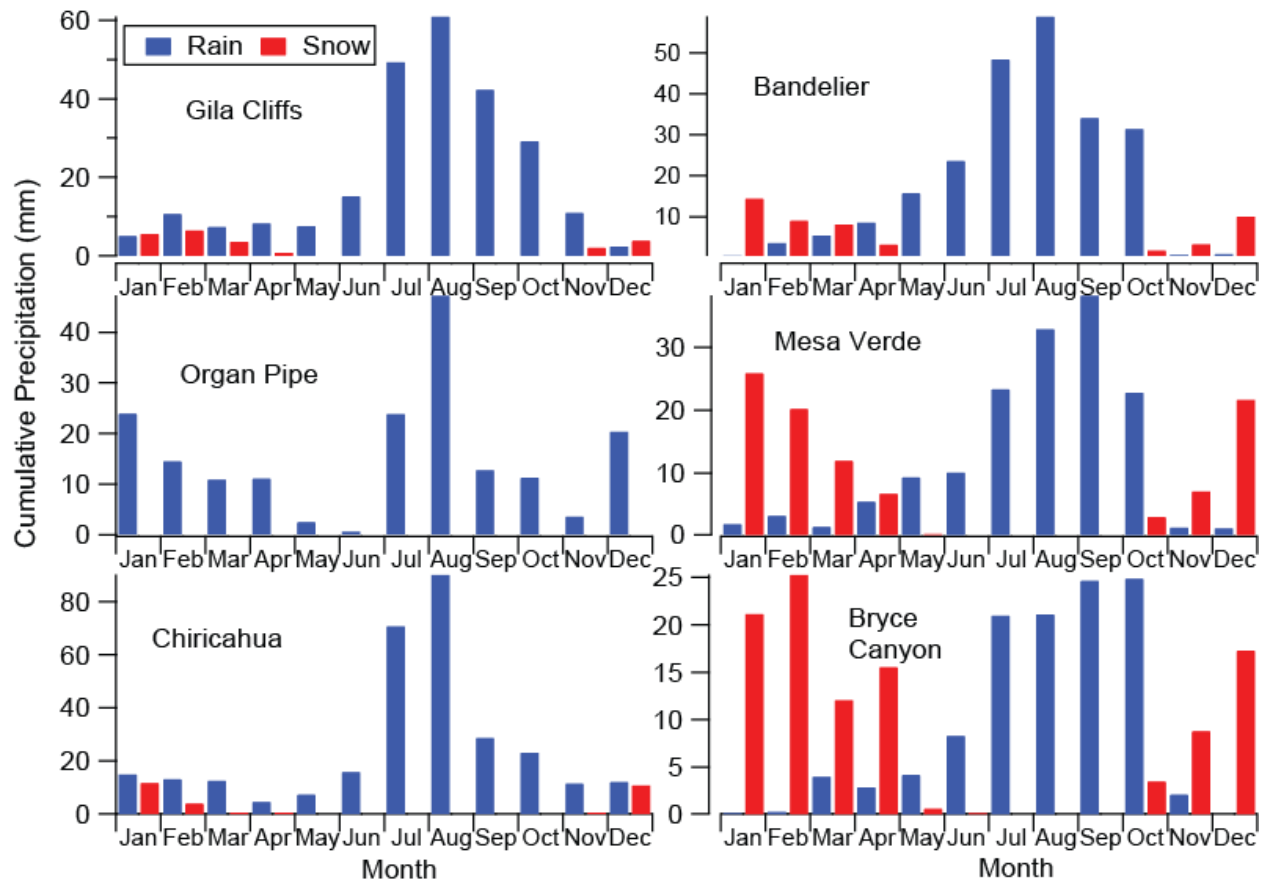
1426  
 1427  
 1428  
 1429  
 1430  
 1431  
 1432  
 1433  
 1434  
 1435  
 1436  
 1437

**Fig. 5.** Average monthly mass fractions of selected  $PM_{2.5}$  constituents for all six IMPROVE sites and for four seasons. The labels for each color in the top left pie are the same for the other pies. Also reported are average  $PM_{2.5}$  and coarse aerosol concentrations in units of  $\mu g m^{-3}$ , the concentration ratio of OC to  $PM_{2.5}$ , and the concentration ratio of the sum of the seven inorganic components of the pies ("Inorg") relative to  $PM_{2.5}$ . These results are based on data ranges in Table 1 for each site.



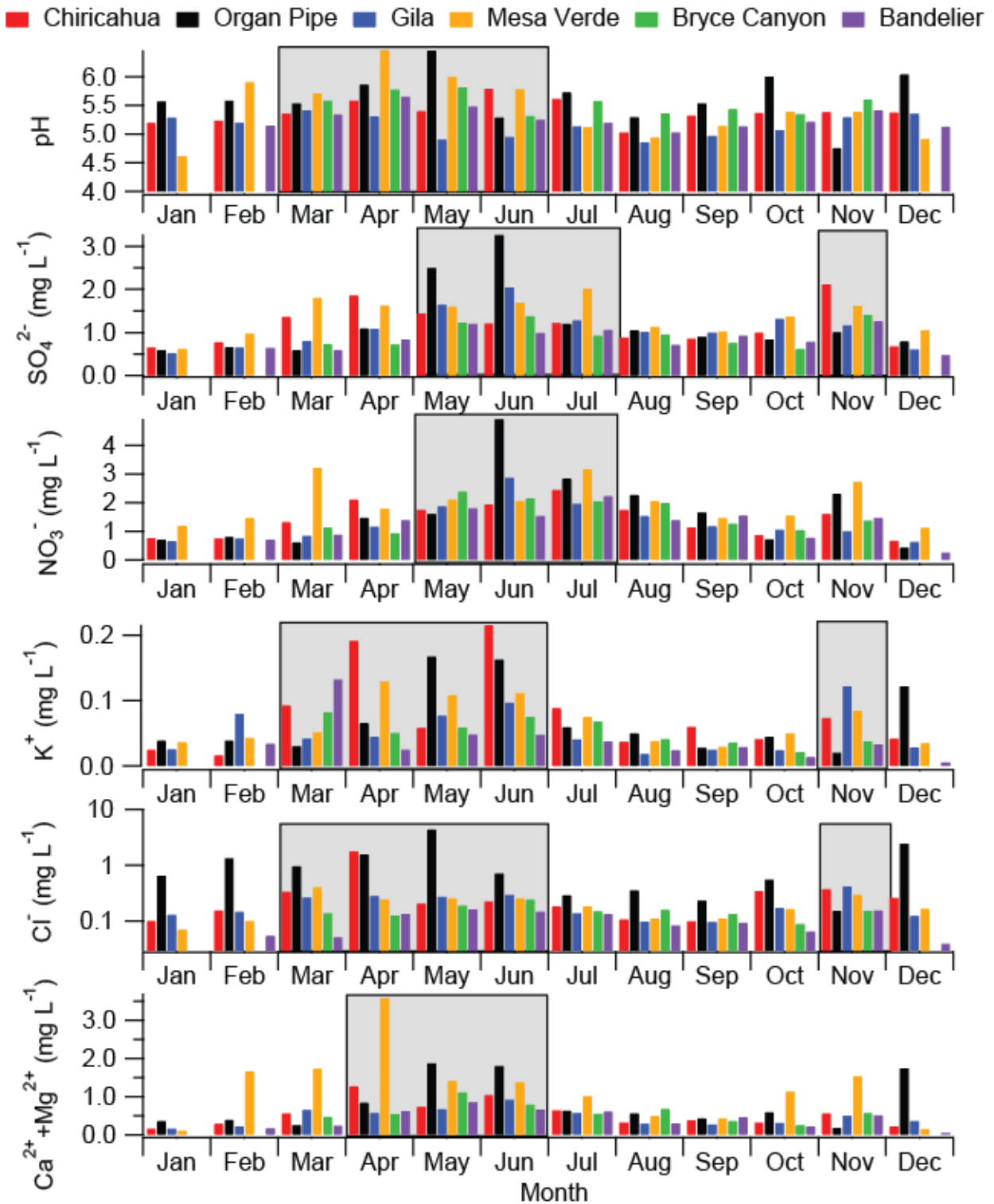
1438  
 1439  
 1440  
 1441  
 1442  
 1443

**Fig. 6.** Average monthly PM<sub>2.5</sub> constituent mass concentrations at six EPA IMPROVE sites. Shaded regions represent when maxima are observed for individual or groups of sites. These results are based on data ranges shown in Table 1 for each site.



1444  
 1445  
 1446  
 1447  
 1448  
 1449  
 1450  
 1451  
 1452  
 1453  
 1454  
 1455  
 1456  
 1457  
 1458  
 1459  
 1460

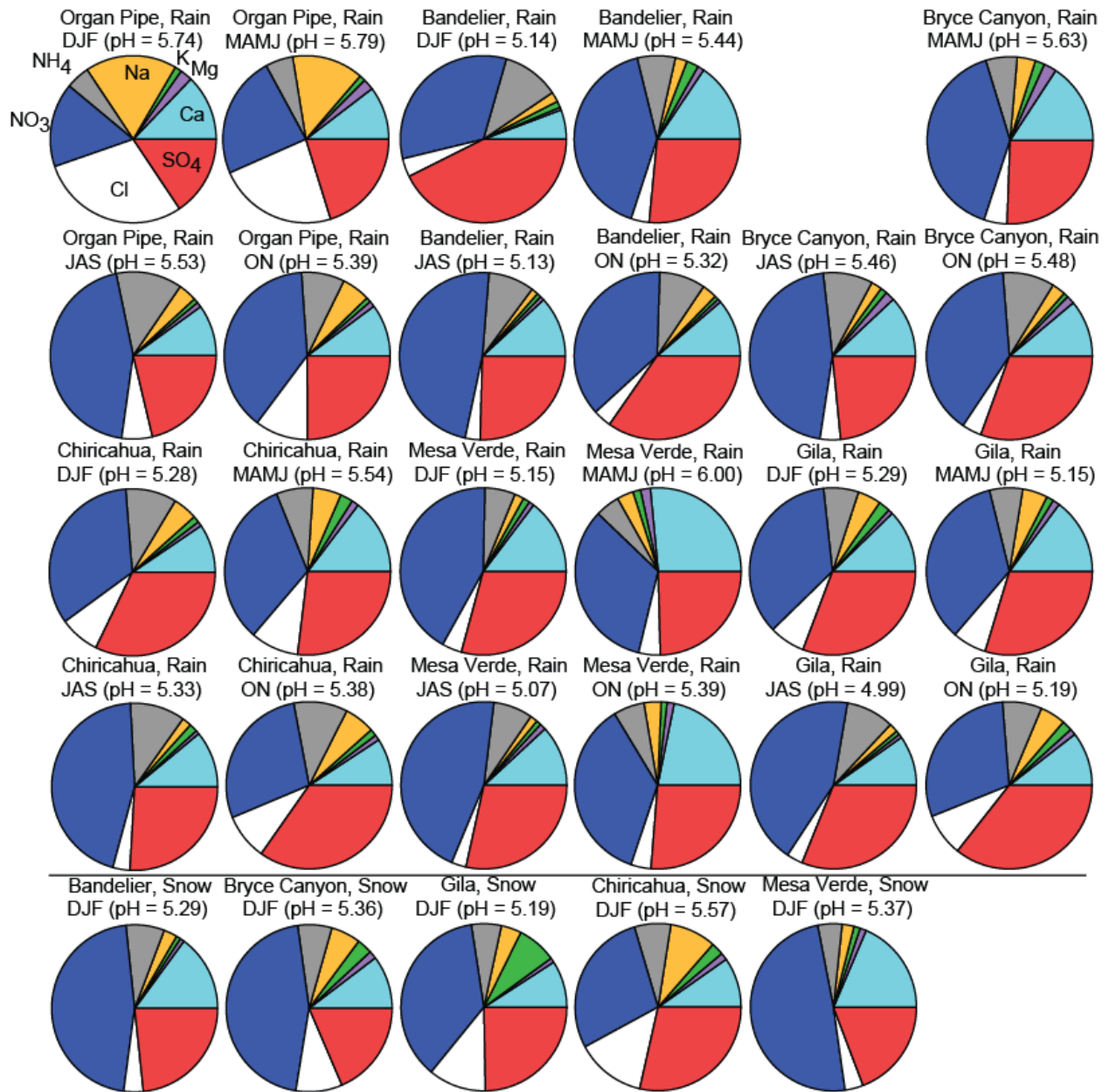
**Fig. 7.** Average monthly precipitation accumulation at the six NADP/NTN sites over the data ranges shown in Table 1.



1461  
 1462  
 1463  
 1464  
 1465  
 1466

**Fig. 8.** Annual pH and concentration profiles for rain in the Southwest. Shaded regions represent when maxima are observed for individual or groups of sites. These results are based on data ranges shown in Table 1 for each site.

1467  
1468



1469  
1470  
1471  
1472  
1473  
1474  
1475

**Fig. 9.** (Top four rows) Summary of pH and chemical mass fraction data for rain during different periods of the year. (Bottom row) Snow pH and chemical mass fraction data for DJF, which is the season with the most snow data available. The labels in the top left pie are the same for the other pies. Note that during DJF there is no rain data for Bryce Canyon or snow data for Organ Pipe.